APPLIED SPECTROSCOPY REVIEWS
Vol. 39, No. 0, pp. 1–51, 2004

Pulsed Nozzle Fourier Transform Microwave Spectrometer: Advances and Applications

E. Arunan,* Sagarika Dev, and Pankaj K. Mandal

Department of Inorganic and Physical Chemistry, Indian Institute of Science, Bangalore, India

CONTENTS

*Correspondence: E. Arunan, Department of Inorganic and Physical Chemistry, Indian Institute of Science, Bangalore 560 012, India; Fax: +91-80-2360-1552; E-mail: arunan@ipc.iisc.ernet.in or earunan@rediffmail.com.

DOI: 10.1081/ASR-120030906 0570-4928 (Print); 1520-569X (Online)

ABSTRACT

The pulsed nozzle Fourier transform microwave (PNFTMW) spectrometer was developed by Balle and Flygare [A new method for observing the rotational spectra of weak molecular complexes: KrHCl. J. Chem. Phys. **1979**, *71* (6), 2723–2724 and **1980**, *72* (2), 922–932] in 1979. The design, fabrication, and operation of this spectrometer are complicated and it has largely remained a research laboratory tool till now, though a portable spectrometer for routine analytical applications has been developed at the National Institute for Standards and Technology [Suenram, R.D.; Grabow, J.-U.; Zuban, A.; Leonov, I. A portable pulsed-molecular-beam Fourier-transform microwave spectrometer designed for chemical analysis. Rev. Sci. Instrum. **1999**, *70* (4), 2127–2135]. However, the potential for extracting fundamental information about any chemical species, such as, molecules, radicals, ions, or weakly bound complexes between any of them including atoms, has been quite significant. It is evident from the fact that more than 25 laboratories around the globe have built this spectrometer, some in the recent past. Contributions from all these laboratories have widened the horizon of PNFTMW spectrometer's applications. This review summarizes the advances in design and the recent applications of this spectrometer. We also define an electrophore, as an atom/

molecule that generates an electric dipole moment by forming a weakly bound complex with a species having zero electric dipole moment. The electrophore, thereby, enables structural determination using rotational spectroscopy, as in the case of Ar_2–Ne, with Ne as the electrophore. Also, it can introduce a dipole moment about a principal axis where none existed before, such as in Ar–$(H_2O)_2$, enabling the observation of pure rotational transitions for several tunneling states.

Key Words: FTMW spectroscopy; van der Waals complexes; Hydrogen bonding; Electrophore.

I. INTRODUCTION

Microwave spectroscopy has traditionally been used in precise structural determination of small molecules in the gas phase.[1–5] Only gaseous molecules or liquid and solid molecules with finite vapor pressure could be studied. This limited the usefulness of microwave spectroscopy and in the 1970s, interest in this area was steadily declining. The development of pulsed nozzle Fourier transform microwave (PNFTMW) spectrometer by Balle and Flygare[6] changed the scenario completely and since then there has been a renaissance in this area. This year marks the 25th anniversary of the PNFTMW spectrometer. It all started on 19th May 1979, with the observation of a strong transition from the weakly bound Ar–HCl van der Waals complex, which had previously been studied using the molecular beam electric resonance technique.[7] The spectrometer has become popular due to its unique characteristics of providing high sensitivity and resolution, simultaneously. From the first report,[8] studies on weakly bound complexes such as hydrogen bonded or van der Waals complexes have dominated the field. However, several recent experimental advances have enabled applications in various areas and this review attempts to highlight some of them.

There have been several reviews and book chapters written on the PNFTMW spectrometer,[9–15] the last of which appeared in 1996.[13] Novick hosts a website containing a comprehensive bibliography of all the weakly bound complexes that have been studied with this and other techniques.[16] Kisiel hosts a website that gives access to all the research groups currently using this and related techniques.[17] Both these websites are useful references in addition to the reviews referred above, especially for keeping track of the recent progress. In this review, we discuss the original design of this spectrometer and highlight all the general and specific changes that have been introduced by various practitioners of the field. We also discuss the diverse applications of this versatile spectrometer, but limit ourselves to literature

published mostly in the last decade, for applications. Though, every attempt has been made to highlight important advances, due to space and time constraints, it is likely that we have missed some important contributions.

II. DESIGN AND OPERATION

A. Original Design and Operation

The schematic diagram of the PNFTMW spectrometer designed by Balle and Flygare[6] is given in Fig. 1. It mainly consisted of (1) Fabry–Perot cavity with two highly polished mirrors housed in a vacuum chamber, (2) supersonic nozzle to prepare a molecular beam, (3) pumping system to produce the vacuum (typically 10^{-6} mbar) and pump out the gas mixture from the pulsed valve, and (4) rf and microwave electrical circuits for polarization of the gas sample and detection of emission from the emitting species. The mirrors were typically large (30–50 cm in diameter) which necessitated large vacuum chambers. The radius of the mirror (a) and its radius of curvature (R) determine the lower frequency limit for the Fabry–Perot cavity, at which the Fresnel number is unity as given below (λ is the wavelength):

$$\frac{a^2}{R\lambda} = 1 \tag{1}$$

Today the lower frequency limit is typically 3 GHz in several laboratories and the mirror diameter is 50 cm. The pulsed molecular beam traveled perpendicular to the Fabry–Perot axis and the pumping speed determined the residence time of the sample within the cavity. Both radiation and the gas mixture are pulsed into the evacuated cavity. The bandwidth of the source is typically less than a MHz and if the sample has any rotational transitions within this bandwidth, it is polarized. The emission from the polarized sample is detected in time domain through a double super-heterodyne mixing scheme and digitized. Fourier transformation of the time-domain signal gives the frequency spectrum. As the spectral range (8–18 GHz in the original spectrometer) is very broad compared to the bandwidth of the cavity, laborious scanning is needed. Two separate microwave oscillators, master and local, were used for the heterodyne detection. Phase stabilization of the master and the local oscillators was a tedious process. Several laboratories followed this design initially and used two oscillators.[18–23] The original design used waveguide components and hence needed to be operated within an octave band (X 8–12 GHz and Ku 12–18 GHz). Since then, various improvements in design have been achieved by different groups and they are discussed next.

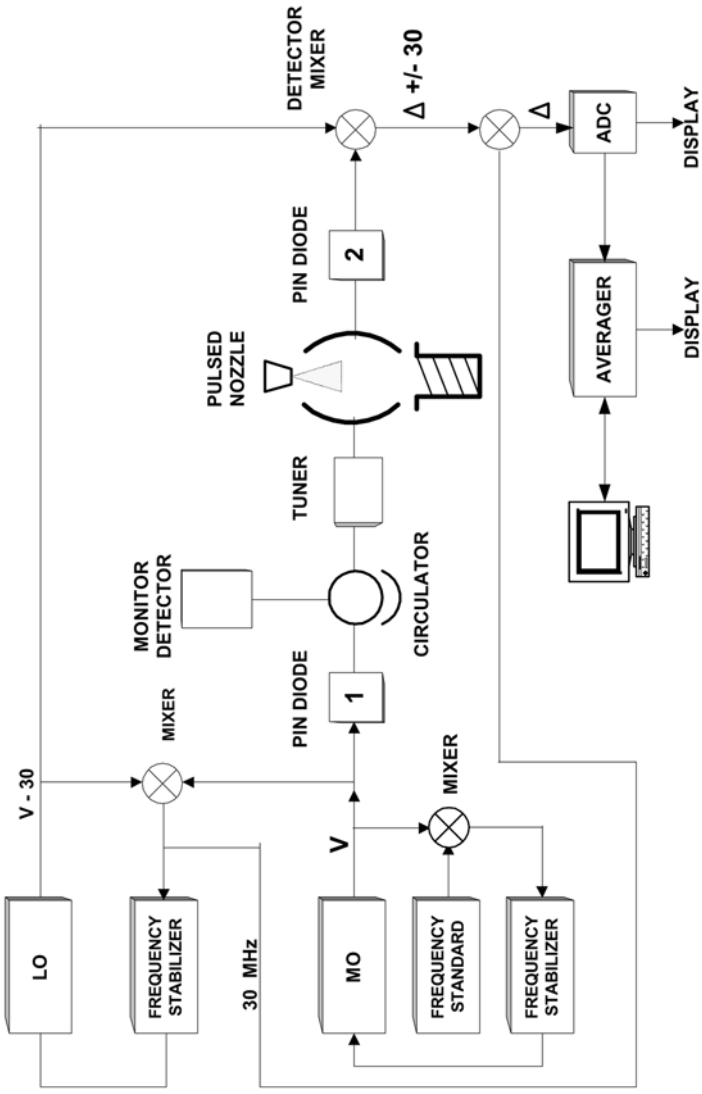

Figure 1. Original configuration of the Balle–Flygare spectrometer. LO, Local oscillator; MO, master oscillator. *Source:* Figure redrawn with permission from American Institute of Physics, Ref.[8].

B. Significant Advances in the General Design

The first major modification was introduced by Suenram and coworkers from National Institute of Standards and Technology[24] and Kruger and Dreizler at Kiel.[25] They used a single side band mixer (SSBM) to produce the second microwave source instead of using two MW oscillators. Only one microwave source, typically a commercial synthesizer, was used as the local oscillator (LO). The master oscillator (MO) was produced by mixing an RF (typically 30 MHz) with the LO in an SSBM. This eliminated the need for complicated phase stabilization. Moreover, the LO was used either for polarization or for detection through a single pole double throw (SPDT) pin-diode switch, which routes it to an SSBM or an image rejection mixer, alternately. Thus, it also eliminated the MO from the cavity, when it is not needed. In the original design, the MO was always present in the Fabry–Perot cavity leading to a DC offset at the base band output. The second important modification was introduced by Grabow and Stahl.[26] They moved the pulsed nozzle from top of the vacuum chamber to behind one of the mirror. Both the microwave and molecular pulses were coaxial in this arrangement and this led to a significant increase in the residence time of the sample in the cavity. This, in turn, reduced the line width to a few kHz enabling the observation of small hyperfine splitting. For example, Fig. 2, shows the ^{13}C spin-rotation interaction of only 4.9 kHz well resolved in the O^{13}CS, $J = 0 \rightarrow 1$ transition, obtained in our spectrometer. Figure 3 shows the same transition for the parent OCS, showing a line width of 2.8 kHz only. Thirdly, the spectrometer operation was completely automated both in Urbana[27] and Kiel[28] in 1990. Other major changes were the use of coaxial cables throughout the frequency range and the use of ultra-broadband microwave components. These ensured that the spectrometer could be operated throughout the range without change of components.[29] All these changes have been implemented in most of the newly fabricated spectrometers.[30–40] A schematic diagram of the spectrometer that is used in our laboratory[40] is shown in Fig. 4 and it is typical of the PNFTMW spectrometer today.

C. Specific Changes in Design

1. Frequency Range: Extending in Both Directions!

In addition to the general changes that are highlighted above, there have been several specific changes introduced in the design of PNFTMW spectrometer for various applications. The frequency range has been extended in

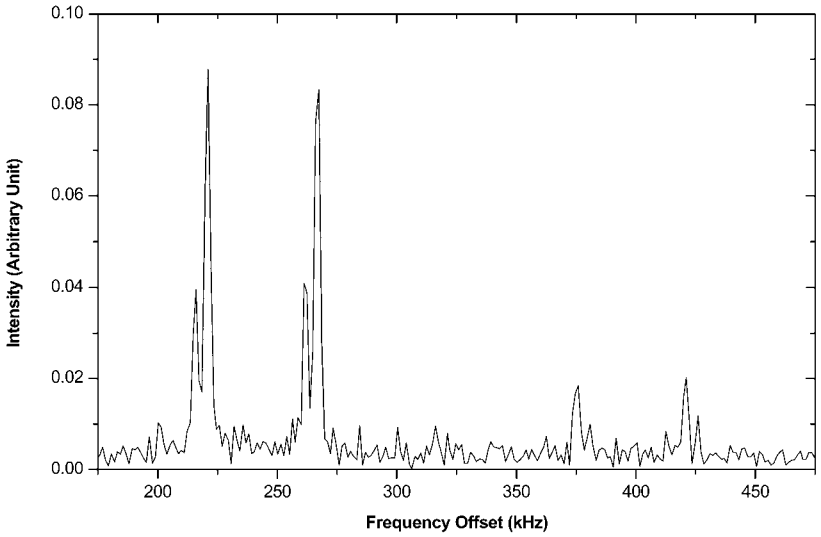

Figure 2. $J = 0 \rightarrow 1$ transitions for $O^{13}CS$ observed in natural abundance at 12123.8437 MHz. In addition to the Doppler doubling, hyperfine splitting of 4.9 kHz due to the ^{13}C spin rotation interaction can be observed. MO frequency was at 12123.6 MHz. *Source:* Figure reproduced with permission from Current Science, Ref.[40].

both directions and today, there are spectrometers operating from 1 GHz[41] to 40 GHz.[42] The high frequency limit could be extended with similar confocal cavity as used by Balle–Flygare. Availability of coaxial cables with low loss has largely helped in this development. However, for extending to lower frequency, say 1 GHz, adapting a confocal Fabry–Perot cavity would result in mirrors with very large diameter according to Eq. (1). This, in turn, will raise the chamber size and the load on the pumping system. Instead, the Kiel group has opted for cylindrical resonator. The estimated low-frequency cutoff is 914 MHz. This spectrometer has been used to observe a transition at 1325.17 MHz, which may yet be the lowest frequency transition observed with such spectrometers. After the initial report, it appears that, there has not been many more studies reported at lower frequency range. In the studies on weakly bound complexes, especially for the larger clusters, the low frequency limit is quite important. Hence, it is likely that, there will be more interest in the low frequency range in future. The cylindrical resonator, theoretically, has no upper frequency limit. Earlier, Emilsson used aluminum collars around both mirrors to keep the electric field within the cavity at frequency below 2 GHz, with 50 cm diameter mirrors.[43] Use of a Balun

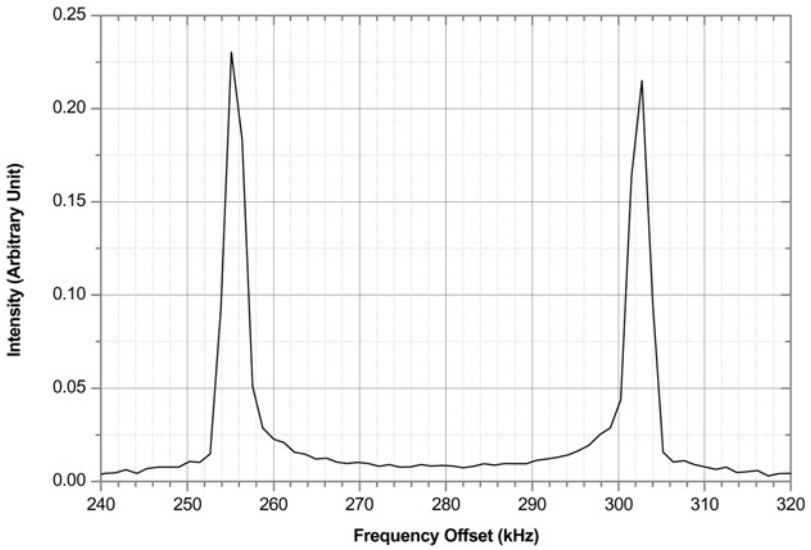

Figure 3. $J = 0 \rightarrow 1$ transition of OCS at 12179.9789 MHz with MO frequency at 12179.7 MHz. The line width is 2.8 kHz. *Source:* Figure reproduced with permission from Current Science, Ref.[40].

transformer as the antenna for transmitting and receiving the microwave power also helped in this effort. Sharp resonances could be observed down to 1.7 GHz. This setup was used to observe the $J = 0 \rightarrow 1$ transition of the $Ne{-}C_6H_6{-}H_2O$ trimer at 1918.6911 MHz.[43]

2. Size of the Spectrometer: Towards a Portable Spectrometer for Chemical Analysis

Two compact versions of the spectrometer have been reported by Harmony et al.[34] and Suenram et al.[44]. Harmony used 10 cm diameter mirror and the lower frequency limit was $\sim$15 GHz. The NIST group used 19.5 cm diameter mirror and could use the spectrometer down to $\sim$8 GHz. While Harmony's main objective was in making the spectrometer compact without loosing the sensitivity, the NIST group's objective was in building a spectrometer for routine analytical applications, especially for automobile emission analysis. Hence, the nozzle was designed to have two inlets, one for a standard and one for a reference. This spectrometer could be operated in various modes suitable for routine analysis. The S/N ratio for the compact instrument was roughly $1/2$ per unit time compared to the larger spectrometer

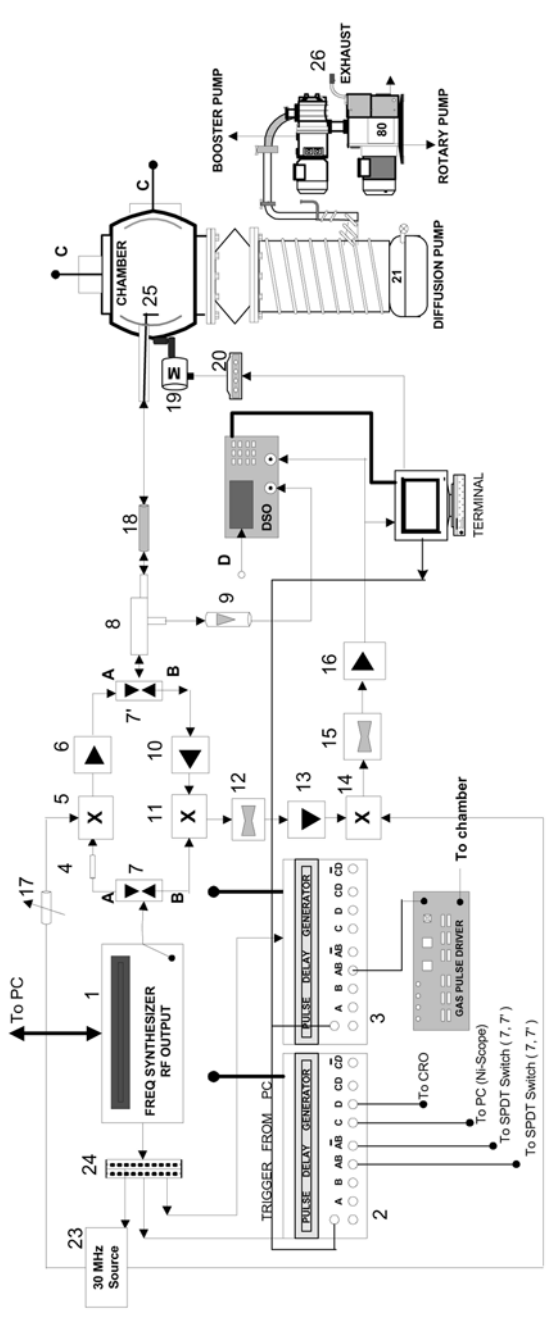

Figure 4. Schematic diagram of the PNFTMW spectrometer at the Indian Institute of Science. 1, Frequency synthesizer (Hewlett Packard, HP83630L); 2 and 3, delay generator (SRS DG535); 4, microwave attenuator (HP, 8493C, 3dB); 5, SSB mixer (Miteq, SMO-226LC1A); 6, medium power amplifier (Miteq, JS3-02002600-5-7A); 7, MW SPDT switch (Sierra Microwave, 0.5-26.5 SFD0526-000); 8, direction coupler (Narda, 1.7-26.5–4227–16); 9, diode detector (Narda, 0.01-26.5–4507); 10, low noise amplifier (Miteq, JS4-02002600-3-5P); 11, image rejection mixer (Miteq, IRO-0226LC1A); 12, band pass filter (Mini Circuits, BBP-30); 13 and 16, RF amplifier (Mini Circuits, ZFL-500LN); 14, RF mixer (Mini Circuits, ZAD-1); 15, low pass filter (Mini Circuits, BLP-5); 17, attenuator (Mini Circuits, ZAFT-51020); 18, blocking capacitor (HP, 11742A); 19, stepper motor; 20, motor driver; 21, diffusion pump and 22, rotary pump (Vacuum Techniques, Bangalore, India); 23, 30 MHz function generator (Stanford Research System, DS345); 24, distribution amplifier (Stanford Research System, FS710); 25, antenna. *Source:* Figure reproduced with permission from Current Science, Ref.[40].

at NIST. This spectrometer can be operated in four different modes. Besides the standard operational mode, automated scanning mode has been developed. The third mode of operation has been developed for continuous process monitoring. In this mode, the spectrometer is tuned to the desired frequency and a preset number of pulses averaged. The resulting signal intensity is determined and displayed in a bar graph in the computer screen. Thus, a concentration vs. time plot is generated, which quantifies the species as well. The fourth mode allows repetitive sampling of a number of chemicals. A number of chemicals can be selected and the machine can be operated to carry out the analysis for each chemical species using a predetermined frequency and optimized pulse parameters for each chemical species. Finally, the measured concentration data for each molecular species is stored in a file. This mode helps to identify and quantify analytes in a sample without prior separation. Though the technique is less sensitive than usual gas chromatography or mass spectrometer, it has several advantages. An individual rotational transition is observed and it provides unambiguous chemical identification. Even, conformers of identical mass can also be identified separately. Table 1 gives the detection limit estimated by the NIST group for various compounds. The Kiel group has reported the development of a PNFTMW spectrometer for analytical purposes as well.[45]

3. Variation in Nozzle Design

Several variations in the nozzle design have been devised for different applications. Firstly, high temperature nozzles are used for studying less volatile species, pyrolysis products, and vibrationally excited states. A storage reservoir has been added, either for liquids or solids such that the carrier gas flows over the sample before expansion. Fast mixing nozzles are used for producing weakly bound complexes between reactive species. Electric discharge nozzles are used for producing transient species, radicals, ions, and their complexes. Laser evaporation of a solid rod, located in front of the nozzle, has been used for producing metal/metal salts for analysis as well. This section looks at the design of these nozzles and their applications.

a. High Temperature Nozzle

Most of the laboratories use commercial pulsed nozzle (Series 9 from General Valve Corporation being the most common) suitable for room temperature applications only. Commercial valves are available for operation up to 200°C. Due to the instability of the various sealing components at higher temperature, it is not possible to go beyond this temperature. Initial attempts for raising the temperature were done by extending the plunger in the valve and using metal O-rings. Shea and Campbell used copper O-ring to

Table 1. Detection limits for various compounds using FTMW spectroscopy.[a]

Compound	Detection limit (nanomol/mol)
Acrolein	0.5
Carbonyl sulfide	1
Sulfur dioxide	4
Propionaldehyde	100
Methyl-*t*-butyl ether	65
Vinyl chloride	0.45
Ethyl chloride	2
Vinyl bromide	1
Tolune	130
Vinyl cyanide	0.28
Acetaldehyde	1
Propylene oxide	11
Para-tolualdehyde	150
Methanol	1,000
Benzaldehyde	26

[a]Detection limit based on a 1 min average of accumulated pulses using Ne as the carrier gas. Lower concentration can be detected by extending the time.
Source: From Ref.[44]. Table reproduced with permission from American Institute of Physics.

attach the pulsed valve to a small furnace storing Hg.[46] They reported the first application of a high temperature nozzle with PNFTMW spectrometer to study Hg–HCl complex. Endo et al. used an aluminum O-ring with an automobile fuel injector[47] and reported results on Hg–OCS. These types of nozzles could work up to 500°C.

Emilsson overcame the problem by putting a furnace below the nozzle and cooling the top of the furnace by water circulation. The nozzle is still kept at room temperature, but the gas mixture is heated before the expansion occurs.[48] This design helped in raising the temperature limit to 1100°C. Gutowsky's group used this high temperature nozzle, shown in Fig. 5, to resolve a long-standing controversy about the silicon–carbon double bond length.[48] They pyrolyzed 1,1-dimethylsilacyclobutane to produce 1,1-dimethylsilaethylene and supersonically cooled it before it could dimerize. The same nozzle was later on used by Arunan et al. to observe Ar/Kr–HCN dimer in which the HCN was in a vibrationally excited state.[49] Evidently, the heating before expansion does not affect the formation of weakly bound complexes. Harmony et al. used a ceramic nozzle in a similar

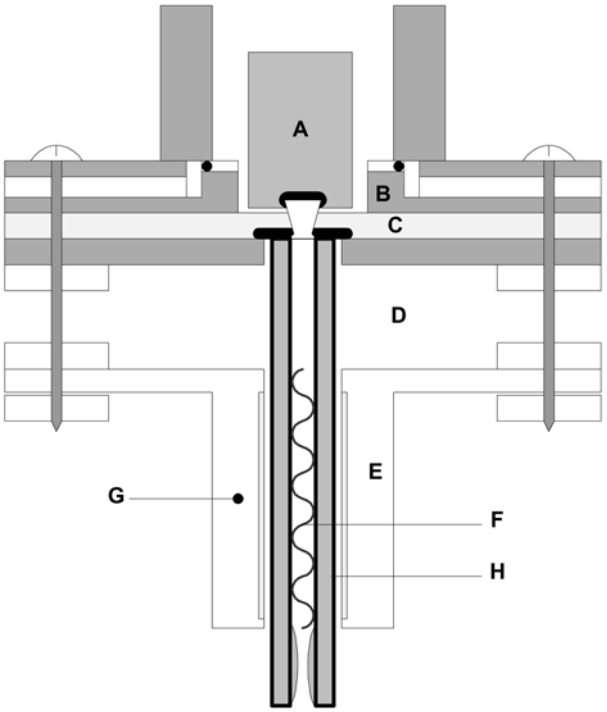

Figure 5. Heated nozzle: A, B, and C, commercial pulsed valve (general valve no: 8-1-900); D, quartz tube; E, cylindrical zone furnace; F, nichrome wire for spoiling the laminar flow of the gas to enhance heat transfer. Appears to have increased the S/N of pyrolyzed products; G, thermocouple; H, heating coil, 3.2 mm i.d. of 18-gauge (0.127 mm) Pt wire in moldable alumina. *Source:* Figure redrawn with permission from American Chemical Society, Ref.[48].

fashion.[34] They observed the rotational transitions for chloroketene from the pyrolysis of chloroacetyl chloride at 800°C. They also observed several vibrationally excited states of OCS. Vibrational cooling is not as efficient during supersonic expansion and this has been exploited in observing the rotational spectrum of vibrationally excited species. Legon and Stephenson used a similar approach to look at pyrolytically produced $CH_2{=}PCl$.[50]

Commercial nozzles with minor modifications have been successfully used by Kukolich et al. to study the rotational spectrum of numerous organometallic complexes, with low vapor pressure. Usually, the nozzle is heated to about 50°C. Recently, they have reported accurate structural determination of tetracarbonyldihydroosmium[51] and tetracarbonyldihydroiron.[52] The

distances between the two hydrogen atoms were determined to be 2.40(2) Å and 2.19 Å, respectively. This is much longer than what is expected for a dihydrogen complex (0.8 Å). This clearly identified both these complexes as classical dihydrides rather than η^2 dihydrogen complexes. They have also reported the first molecular structure measurements on bromoferrocene and compared the structural and electronic properties of chloro- and bromoferrocene.[53] The substitution of an electronegative atom (Cl/Br) onto the ferrocene frame leads to an increase (0.04–0.08 Å) in metal to carbon distance compared to ferrocene. The quadrupole coupling constants (χ) for the haloferrocene were very close to those of halobenzene. Evidently, the metal–carbon bonding does not perturb the electric field gradients at the halogen atom, in contrast to the effect of halogen substitution on the interaction between metal and carbon as indicated by a significant increase in metal–carbon distance. Kukolich's group has studied several organometalic compounds including CpNi(NO), $Co(CO)_3NO$, $CpCo(CO)_2$, $CpMn(CO)_3$, $(C_4H_6)Fe(CO)_3$, $HRe(CO)_5$, $HMn(CO)_5$, $HCo(CO)_4$, $(C_6H_6)Cr(CO)_3$, $CpCr(CO)_2NO$, $CpV(CO)_4$, $CpW(CO)_2NO$, CH_3ReO_3, and $(C_2H_2)(CH_3)ReO_2$.

Suenram et al. have recently reported a high temperature nozzle designed with minor modification of the general valve pulsed nozzle.[54] They have used it to study the rotational spectrum of dimethyl methylphosphonate, which is a model compound for nerve agents.

b. Fast Mixing Nozzle

Fast mixing nozzles are used for forming weakly bound complexes between species that react very fast when mixed! The first such nozzle was reported by the Urbana group at the Ohio State symposium in 1988. The details were published later[55] along with results on NH_3–HCN–HF and CO–HCN–HF trimers. Ammonia and HF react fast to produce NH_4F(s), but the use of the fast mixing nozzle, shown in Fig. 6, allowed the study of NH_3–HCN–HF trimer. Studies on these trimers probably showed the first example of microsolvation. The geometry of the trimer was the composite of the X–HCN and HCN–HF dimers. However, there were significant shrinkages in the c.m.–c.m. (center of mass) distances for both X–HCN and HCN–HF moieties. The reduction in c.m.–c.m. distance for X–HCN was 0.070 Å and 0.098 Å, for X = CO and NH_3, respectively, and the corresponding reduction in HCN–HF distance was 0.033 Å and 0.027 Å.

The coaxial mixing nozzle was extensively used by Legon et al. in studying a variety of hydrogen and halogen bonded complexes beginning with $(CH_3)_3P$–HCl[56] and $(CH_3)_3N$–HBr.[57] Legon's comprehensive studies on a series of HX (X = F, Cl, Br, and I) and XY complexes with a Lewis base B have highlighted the similarities between hydrogen and halogen bonds.[15] Hydrogen bonding may no longer be considered unique. By analyzing the

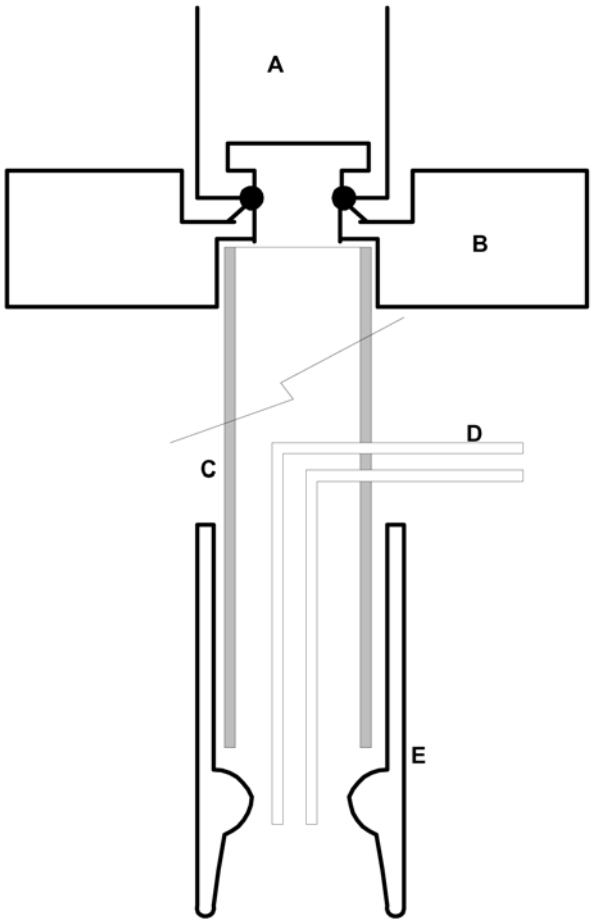

Figure 6. Coaxial mixing nozzle: A and B, plunger and bottom plate of pulsed valve; C, main tube of the valve extension; D, coaxial injection tube; E, adjustable brass sleeve with a Laval type orifice. *Source:* Figure redrawn with permission from American Institute of Physics, Ref.[55].

quadrupole coupling constants for the halogen, Legon has demonstrated the existence of charge transfer complexes in gas phase. While ammonium chloride exists as a hydrogen bonded dimer $H_3N{-}HCl$ in the gas phase, $(CH_3)_3N{-}HCl$ has 62% contribution from the charge transfer structure, $(CH_3)_3NH^+Cl^-$. Table 2 compares the ^{35}Cl nuclear quadrupole coupling constants for $(CH_3)_{3-n}H_nN{-}HCl$ complexes. It may be noted that for the

Table 2. Comparison of ^{35}Cl nuclear quadrupole coupling constants (χ) for $(CH_3)_{3-n}H_nN-HCl$ dimers along with that of HCl, NaCl, and KCl.[a]

Molecule/complex	χ (MHz)	Reference
HCN–HCl	−53.720	[58]
H_3N-HCl	−47.607	[59]
CH_3NH_2-HCl	−37.89	[60]
$(CH_3)_3N-HCl$	−21.625	[61]
NaCl	−5.634	[1]
KCl	<0.04	[1]

[a]For comparison, the χ for ^{35}Cl in free HCl is −67.6189 MHz.
Source: E. Kaiser, J. Chem. Phys. **1970**, *53*, 1686. Evidently, KCl is more ionic than NaCl.

spherically symmetric Cl^- ion, the quadrupole coupling constant will be 0 as observed for KCl. For the $(CH_3)_3N-HX$ (X = Cl, Br, or I) series, the extent of charge transfer increases from Cl to I, with the trimethylammonium iodide existing as the ion pair $(CH_3)_3NH^+I^-$, even in the gas phase.[15]

Leopold et al. have used the fast mixing nozzle to study several complexes of interest in atmospheric aerosol chemistry. Their first report[62] was on H_2O-SO_3, which was expected to be a key intermediate in the formation of atmospheric H_2SO_4. This intermediate could not previously be observed because of the fast reaction between H_2O and SO_3. Their study revealed that the S–O bond length is 2.432 Å in agreement with recent advanced theoretical predictions. Earlier theoretical studies have given S–O bond lengths varying from 1.74 to 2.03 Å. They also observed $H_2SO_4-H_2O$[63] and H_3N-HNO_3[64] adducts using a mixing nozzle. It has been concluded from the structural analysis that the $H_2SO_4-H_2O$ adduct has a strong hydrogen bond between the H from H_2SO_4 to the O of H_2O with an O–H distance of 1.645(5) Å and a weak hydrogen bond between the H of H_2O and the O from the S═O group of H_2SO_4, see Fig. 7. The hydrogen bond length in the latter case is 2.05(1) Å. In water dimer, the O–H hydrogen bond length is 2.02 Å[65] and the "weak hydrogen bond" noted by the authors is more likely a typical hydrogen bond. It is likely that the "strong hydrogen bonding" noted by Leopold et al. actually involves partial ion-pair formation, i.e., $H_3O^+HSO_4^-$. Determining the electric quadrupole moment of ^{17}O in $H_2^{17}O-H_2SO_4$ could provide crucial evidence about ion-pair formation. The hydrogen bond length observed in H_3N-HNO_3[64] is significantly shorter than that in the corresponding HCl and HBr complex. It appears that, this could be due to the increasing contribution from ion-pair states ($H_4N^+X^-$, X = Cl, Br, NO_3). The ^{14}N (of NH_3) quadrupole coupling constant should give vital

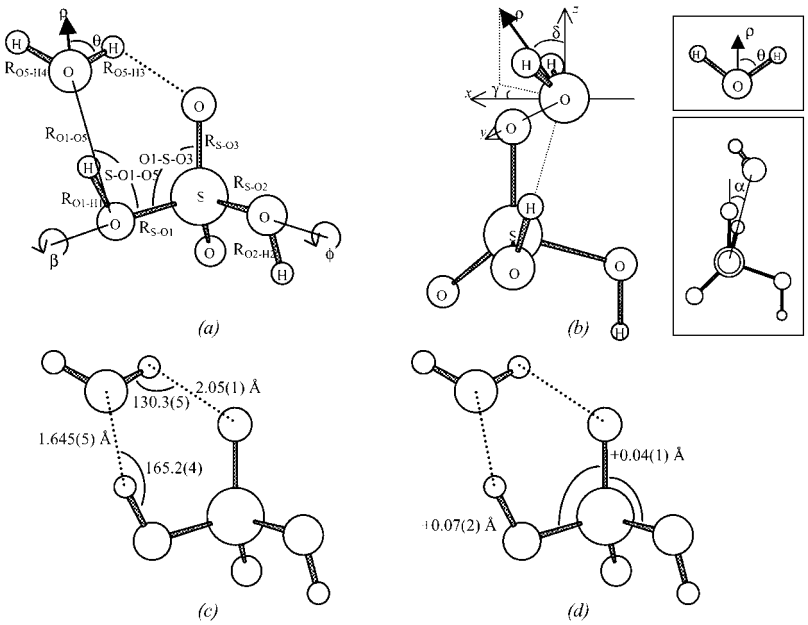

Figure 7. Four views of the sulfuric acid–water complex, emphasizing (a) bond lengths and bond angles within the monomers; (b) intermolecular parameters specifying the relative orientation of the monomers (α is the O5–O1–S–O3 dihedral angle; a positive value of δ and a negative value of γ are drawn; see text for discussion); (c) chemically interesting features of the experimentally determined structure; and (d) changes in the sulfuric acid monomer structure upon complexation (value in H_2SO_4–H_2O minus value in H_2SO_4 monomer). The authors have interpreted the two hydrogen bonds observed as weak [2.05 Å in (c)] and strong [1.645 Å in (c)]. It may be noted that the bond distance observed for the "weak" hydrogen bonding is nearly identical to a typical hydrogen bond length as observed in $(H_2O)_2$. *Source:* Figure reproduced with permission from American Chemical Society, Ref.[63].

information again. However, the authors have attributed the difference in quadrupole coupling constant between free NH_3 and the complex to vibrational averaging only. Interestingly, detailed analysis of ^{14}N quadrupole coupling constant in HNO_3 has led to the conclusion of significant electronic distortion in HNO_3.

Leopold et al. have used the fast mixing nozzle to study HCN–HCN–BF_3[66] and HCN–HCN–SO_3[67] as well. In both these cases, there is a significant decrease in the c.m.–c.m. distance between HCN and BF_3/SO_3 compared to the "free" dimer. Table 3 compares the N–Y and N–H distances for various HCN–HCN–Y trimers that have been studied. From this, they

673 ***Table 3.*** Bond length changes for complexes $HCN\cdots HCN-Y$.[a]

Complex	ΔR(N–Y)	ΔR(N···H)	Reference
$HCN\cdots HCN-BF_3$	0.174	0.045	[66]
$HCN\cdots HCN-SO_3$	0.107	0.017	[67]
$HCN\cdots HCN-CO_2$	0.052	0.004	[68]
$HCN\cdots HCN-HCF_3$	0.042	0.030	[68]
$HCN\cdots HCN-HF$	0.043	0.069	[68]
$HCN\cdots HCN-HCl$	0.062	0.054	[68]

[a]Distance in the dimer minus the distance in the trimer.

Source: Table reproduced with permission from American Chemical Society (Ref.[67]).

have concluded that the weak, closed shell interactions (that between two HCN or HCN and HX) remain weak, but incipient donor–acceptor bonding (between HCN and BF_3/SO_3) is driven forward by forming an adduct with a nearby molecule. It has been called microsolvation! It would be interesting to study $H_2O-HCN-BF_3$ to look at microsolvation by "the solvent."

c. Pulsed Discharge Nozzle

A significant change in the nozzle design was the addition of the electric discharge right after the nozzle, which is popularly known as pulsed discharge nozzle (PDN). This has made possible studies of ions, radicals, and their complexes. Several laboratories added this feature in the early nineties[69–71] and a casual perusal of literature today would suggest this to be the most important addition to PNFTMW spectrometer. From the beginning, linear carbon chains have been the major targets for investigations with PDN-FTMW spectrometers. The PDN used by Ohshima and Endo[72] is shown in Fig. 8. This has been used for the observation of several linear carbon radical species including C_3S, C_2N, C_2Cl, C_2S, NCCS, HC_4N, CH_2CCH, HC_3S, and HC_4S. Endo et al. have also studied rare gas-ion/radical complexes such as $Ar-SH$[73], $Ar-HN_2^+$, and $Kr-HN_2^+$[74] using PDN, recently. They have earlier reported studies on Ar–OH, Kr–OH, $Ar-HCO^+$, and $Kr-HCO^+$, as well. These studies provide useful information as interactions between charged species and rare gas are stronger compared to the interaction between neutral molecules and rare gases.

McCarthy, Thaddeus et al. have made extensive use of the PDN-FTMW spectrometer for studies on carbon chains and rings[75] and sulfur–carbon chains.[76] Their main focus is on laboratory studies on molecules/radicals of astrophysical interest. Most of the astrophysical molecules with more than four atoms are "organic" involving carbon–carbon bonds. Systematic

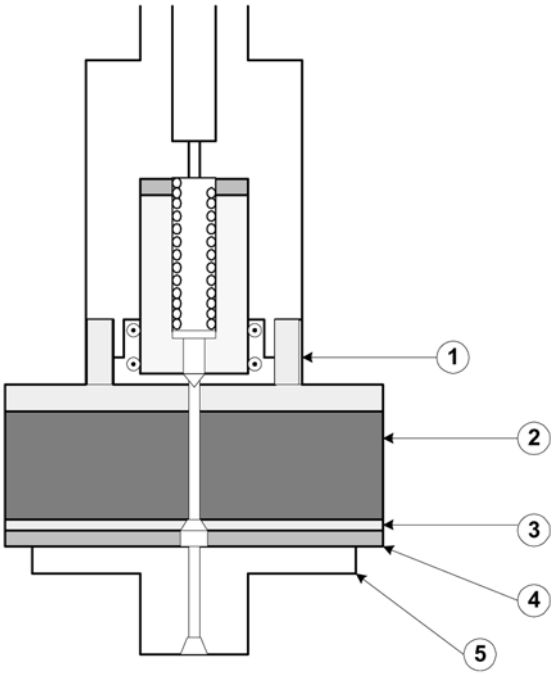

Figure 8. Pulsed discharge nozzle. 1, solenoid valve (General Valve Co.); 2, plastic separator with a 1.0 mm φ hole (10 mm thick); 3, SUS plate with a 1.0 mm φ hole (1 mm thick); 4, teflon separator with a 3.0 mm φ hole (2 mm thick); and 5, brass block with a 1.5 mm φ hole 10 mm in length. *Source:* Figure redrawn with permission from Academic Press, Ref.[72].

studies on many of these species from their laboratory highlight the importance of PDN-FTMW spectrometer. Within a 4 year period, they could look at 77 reactive species (see Figure 3 of Ref.[75]), which could not be detected earlier. This led the authors to comment that "the laboratory astrophysics of the radio molecules is complete in the sense that the lines of astronomical interest have either been measured directly or can be calculated to high precision." However, in further pursuit of observing short lived, low abundant species of astrophysics interest, a cryogenic PDN-FTMW spectrometer has been built recently.[77] In this spectrometer, the cavity mirrors are cooled to liquid N_2 temperature leading to significant reduction in system noise temperature. Against the theoretical improvement by a factor of 60 in S/N ratio compared to the room temperature spectrometers, the cryogenic spectrometer has achieved a factor of 26. This limit is mainly due to the commercial low

noise amplifier having a noise temperature of 181 K and, one can be sure that we will continue to see improvements in this front.

The PDN has been used by Gerry et al. to observe the unstable molecules FBO, ClBO, and FBS, recently.[78] Kukolich et al. have obtained the rotational spectrum of *o*-benzyne with the PDN-FTMW spectrometer very recently.[79]

d. Laser Ablation Source

Laser ablation of a rod placed just in front of the nozzle has helped in the studies of refractory materials, reactive and low volatile species, and their complexes. Usually, the rod can be rotated to expose a fresh surface to the laser. First application of this technique was the characterization of SiC_2 by the NIST group.[80] Since then, it has been used in several laboratories to solve many problems that would have otherwise been very difficult, if not impossible. At NIST itself, the laser ablation setup has been used to record the first rotational spectra of metal dioxides ZrO_2[81] and HfO_2.[82] This has yielded accurate structure, electric dipole moment, and quadrupole coupling constants for the dioxides. Both oxides have C_{2v} symmetry, with very similar M–O bond lengths of 1.7764 Å and 1.7710 Å for ZrO_2 and HfO_2, respectively. Both these oxides have nearly the same dipole moments as well, 7.80(2) and 7.92(1) D, respectively. It has been noted that the M–O bond lengths increase by 0.0571 Å and 0.0533 Å when going from MO to MO_2 for M = Zr and Hf, respectively. The bond length is expected to increase from a triple bond for MO to double bond for MO_2.

Gerry et al. were the first to put the nozzle with the laser ablation facility behind the mirror, see Fig. 9, for improved resolution and sensitivity.[83] They have made extensive use of the laser ablation source to look at a variety of noble (coinage) metal halides and their complexes such as Rg–MX[84–86] and OC–MX,[87–89] where M = Cu, Ag, or Au and X = F, Cl, or Br. The MX were formed in gas phase by reacting the laser evaporated M with a halogen source such as SF_6, Cl_2, or Br_2. All Rg–MX complexes were found to have small centrifugal distortion constants and are relatively rigid compared to typical van der Waals complexes. The Au and Cu complexes were stronger than the Ag complexes based on both experimental and theoretical results. The quadrupole coupling constants for the metal showed dramatic changes indicating that the electric charge distribution around the metal changes significantly on complexation with Ar. There is definite evidence that the Rg–Au bond is "chemical" in Rg–AuCl. The quadrupole coupling constant for Au changes from 9.63 MHz in AuCl to −259.8 MHz in Ar–AuCl and −349.8 MHz in Kr–AuCl. However, the quadrupole coupling constant for Cl shows only a moderate change from −61.99 MHz in AuCl to −54.05 MHz in Ar–AuCl. The Ar–Au distance has been determined to be 2.47 Å, very much smaller than the sum of van der Waals radii of Ar and Au (3.60 Å) or even the sum

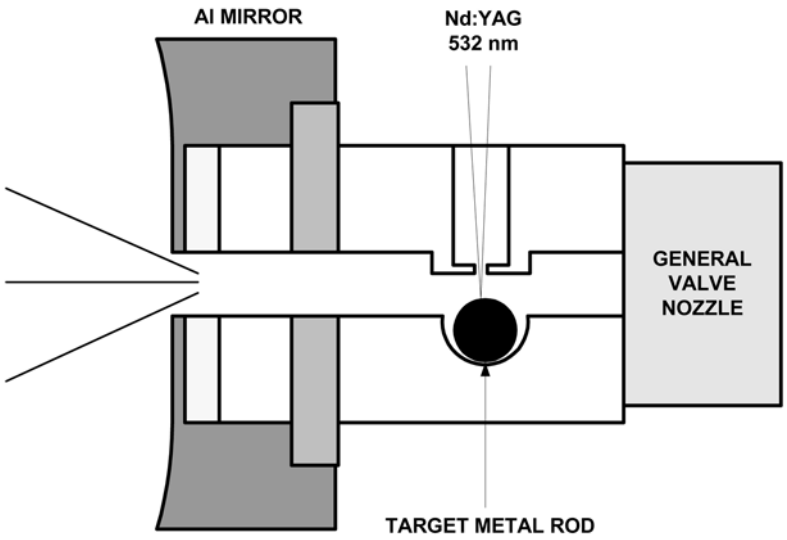

Figure 9. Top view of the laser ablation nozzle cap and part of fixed aluminum mirror. The nozzle cap is mounted slightly off center in the mirror. A motorized actuator (not shown) is located below the plane of the paper. *Source:* Redrawn with permission from Academic Press, Ref.[83].

of the ionic radius of Au^+ and van der Waals radius of Ar (2.9 Å). The binding energy of Ar–AuCl has been evaluated to be 11 kcal mol^{-1}.[86] The Ar–AuCl, thus, becomes the first example for a noble gas–noble metal chemical bond. Table 4 summarizes the quadrupole coupling constants for M and X observed in Rg–MX and OC–MX complexes.

The OC–MX complexes for M = Ag, Au, and Cu could all be prepared with the same ease by the laser ablation technique, though OC–AgX was believed to be difficult to prepare compared to the other two by conventional techniques. Not surprisingly, the OC–MX interactions are much stronger than the Rg–MX interactions. Following OC–MX formation, the quadrupole coupling constants for both M and X show significant changes, see Table 4. For OC–AuCl, the quadrupole coupling constants observed for Au and Cl are −1026.0 and −36.39 MHz, respectively. In all these complexes, the CO bond is shorter than the free CO. Stretching frequencies for free CO is 2138 cm^{-1} while that for OC–MCl (M = Cu, Ag, Au) are 2156, 2184, and 2162 cm^{-1}. Gerry's group has also observed several metal salts including MgS, YX, and AuX (X = F, Cl, Br, I), ScCl, ScF, ZrO, ZrS, MCN/MNC (M = Al, Ga, and In), BiN, and BiP in the last few years.

Table 4. Nuclear quadrupole coupling constants (in MHz) of M, Cl, and Br in various Ar-MX and OCMX.

	OCMX		ArMX		MX	
MX	eQq(M)	eQq(X)	eQq(M)	eQq(X)	eQq(M)	eQq(X)
CuF	75.406	—	38.055	—	21.956	—
CuCl	70.832	−21.474	33.186	−28.032	16.169	−32.127
CuBr	67.534	171.600	29.923	225.554	12.851	261.180
AgCl	—	−28.151	—	−34.486	—	−36.440
AgBr	—	223.902	—	278.888	—	297.047
AuF	−1006.3	—	−333.4	—	−53.31	—
AuCl	−1026.0	−36.39	−259.8	−54.05	9.633	−61.99
AuBr	−999.1	285.09	−216.7	428.5	37.26	492.3

Source: From Ref.[88]. Reproduced with permission from American Chemical Society.

Endo et al. have reported an important study on $(H_2O)_n$–NaCl very recently.[90] These clusters were formed by co-expanding laser ablated NaCl with an Ar stream containing a trace of water. They note that the Na–Cl distance increases by 0.06 Å for $n = 1$ and 0.48 Å for $n = 3$. These results clearly identify the microscopic solvation of NaCl by H_2O and will be very useful for refining the interaction models used in molecular dynamics and Monte Carlo simulations for the description of the ion pair in solution.

4. Stark Effect Measurements

From the early days of PNFTMW spectrometer, measurements of Stark effect have been done,[91] though it is more difficult with this spectrometer than with traditional microwave spectrometers. Usually, the molecular beam had to be perpendicular to the cavity axis. As the cavity is usually large, it required that the flat electrodes were kept far apart. For generating homogeneous fields, these electrodes need to be larger than their separation but should not get too close to the chamber to avoid arcing. As the microwave beam waist increases with decreasing frequency, the Stark effect could be measured only at frequency above 10 GHz or so.[92] The perpendicular arrangement usually leads to weaker signals compared to having coaxial molecular beam and cavity axis. Despite, these inconveniences, several laboratories did use two parallel plates and measured dipole moments for various complexes. Recently, there have been some attempts to improve the design and we limit our discussions to these studies only.

Consalvo reported the first Stark effect measurements with a coaxial arrangement for molecular beam and the microwave cavity.[93] Usually, in this arrangement, it is difficult to get rid of the zero field lines. Consalvo simulated the electric field within the cavity for various designs of the plates and concluded that the plates need to be as longer as practical and the distance between them as shorter. This led to the choice of electrodes with a dimension of 70 cm × 50 cm × 2 mm and these were kept at a distance of 25 cm only. This arrangement worked well as the zero field lines could be eliminated. The homogeneity of the electric field was established. Though, the separation of 25 cm between plates, should allow operations down to 3 GHz according to the calculations, experiments have been reported for frequencies above 10 GHz only.

Emilsson has designed a cubic Stark cage, instead of Stark plates.[92] The Stark cage significantly improved the homogeneity of the electric field. The cage was made of two 1 foot square plexiglass frames held together at the corners by four 2 feet long 3/4 inch diameter aluminum rods. Eleven equally spaced Cu wires were stretched along the long faces of the frame. The field inhomogeneity was estimated to be less than 0.1% based on the experimental line-widths with and without the electric field. This cage could not be used for Stark measurements below 9.5 GHz. However, both $\Delta M = 0$ and ± 1 transitions can be observed as the electric field could be applied in both directions.

Kisiel et al. have reported a novel design of electrodes for Stark effect measurements.[94] They have pointed out the electrical field inhomogeneity present with parallel plate arrangements. Their calculations indicated that field corrections along the expansion direction could be done by attaching simple strips to the edges of the parallel plates. The field correction in the other two directions was achieved by the addition of triangular plates on all four edges.

Grabow et al. have recently come with another novel electrode arrangement.[95] They have used the circular aluminum reflectors themselves as electrodes. Their mirrors are thermally insulated and cooled with liquid N_2 for improving S/N. Thermal insulation also provides electrical isolation and hence the reflectors can be used as electrodes. It is possible to keep both the pulsed valve and the microwave antenna in the same mirror. The other mirror could be set to a static high voltage potential. This arrangement allows only $\Delta M = \pm 1$ transitions to be observed.

5. Double Resonance Experiments

Double resonance experiments have always played an importance role, especially in radio- and microwave spectroscopies.[5,96] Bauder et al. reported the first application of MW–MW double resonance with PNFTMW

spectrometer. It used two pairs of mirrors orthogonal to each other forming two Fabry–Perot cavities.[97] They used this spectrometer to confirm the assignments for some $(H_2O)_2$ transitions and observed two new transitions. The same spectrometer was used later along with ac Stark effect to induce two-photon microwave transitions within a two-level system.[98] One Fabry–Perot cavity was tuned to 8633.5 MHz, which is $1/2$ of the $J = 2$, $K = 2$, $M = 2 \rightarrow J = 3$, $K = 2$, $M = 2$ transition. Two-photon absorption induced a macroscopic polarization which could only decay at 17,267 MHz. The emitted coherent radiation was detected in the second cavity. This was a feasibility study that has not been followed up. The electric field was applied through a cylindrical cage and this affected the quality factor of the cavities. May be some of the newer designs for Stark effect discussed above, could be used with two cavity spectrometers to realize the full potential of two and multiphoton microwave absorption experiments.

Jäger et al. described a microwave–submillimeter wave double resonance spectrometer incorporating a PNFTMW spectrometer.[99] This should prove useful for the studies on van der Waals complexes, as intermolecular vibrations often fall in mmwave region. The availability of tunable coherent backward wave oscillators (BWO) with mW output power has significantly aided in this effort. The BWO enters the MW cavity in a perpendicular direction through a Teflon window and is reflected back by a copper mirror to cross the molecular beam again. If the signal transition is known, then the cavity is tuned in that frequency and a set of transitions are recorded as a function of pump frequencies. If the microwave frequency is not known then a two-dimensional scan has to be done systematically. The projection of 3-D spectrum in submillimeter or microwave axis gives the corresponding frequencies. The best advantage of this double resonance technique is to separate out very closely spaced components of hyperfine lines. As, for example, two hyperfine components in microwave spectrum of $CO–N_2$ are separated only by 5 kHz, which is hard to resolve with a FTMW spectrometer (see Fig. 2, however). But recording the two peaks in two different pump frequencies will separate out the peaks in contour diagram of double resonance technique. It has been used to observe the intermolecular bending vibration of Ar–CO, as well.

Endo et al. have developed MW-optical double resonance spectrometer.[100] The design of the cavity is a typical one, with the supersonic beam from the pulsed discharged nozzle, microwave beam, and the laser beam all mutually orthogonal to each other. The cavity is tuned to the coherent microwave radiation resonant with a particular rotational transition and free induction decay of the emitted radiation is observed while an optical light pulse from laser source is scanned. When the laser light is resonant to one electronic excitation a change in the FID signal is observed. The

MODR spectra of CCS and C_4H radicals have been observed with this spectrometer.

Pate et al. have quite recently developed an IR-FTMW-MW triple resonance spectroscopy technique.[101] This spectrometer has been built to observe the rotational spectrum of a vibrationally excited state. It has been demonstrated by observing the rotational spectrum of $J = 1$ rotational level of propyne in the acetylenic C–H stretch excited state. This development opens the FTMW spectrometer to studies on chemical reaction dynamics.

III. STUDIES ON WEAKLY BOUND COMPLEXES AND COLD MONOMERS

In Section II, many of the applications resulting from the advances in design of the PNFTMW spectrometer were discussed. As indicated earlier, studies on weakly bound complexes have dominated this field from the very first report. The last few years have been no exception with a large number of dimers and trimers added to the list. In this section, we highlight some of the important studies on weakly bound complexes and cold monomers, using PNFTMW spectrometer.

A. Rare Gas Clusters

The PNFTMW spectrometer made observation of the rotational spectrum of rare gas clusters possible. The rare gas dimers are arguably the simplest prototypes for modeling van der Waals interaction. Experimental data on structure and electric charge redistribution would be valuable in developing inter-atomic potential. Gerry et al. reported the observation of Ne–Xe, Ar–Xe and Kr–Xe dimers[102] in 1993 followed by the observation of Ne–Kr and Ar–Kr,[103] Ne_2Kr and Ne_2Xe.[104] In 1995, Grabow et al. presented a detailed study on Ar–Ne dimer[105] arguably the weakest dimer reported till then. Since then, Jäger's group has observed rare gas trimers and tetramers containing Ar and Ne.[106] All these studies were aided by a MW power amplifier as the induced dipole moments for the rare gas clusters were very small. Approximate determination of the dipole moments was carried out by estimating the power required for $\pi/2$ pulse. The dipole moments varied from 0.0029 D for Ar–Ne to 0.014 D for Ar–Xe. For Kr–Xe, one would expect the dipole moment to be larger as both are more polarizable than Ar/Ne, but the estimate was 0.007 D. However, as the authors point out,[103] these are order of magnitude estimates only. In any case,

accurate microwave measurements on rare gas dimers were helpful in refining the pair potentials.[107]

Rare gas-molecule clusters are important as a building block to intermolecular interactions and they have been investigated by PNFTMW spectrometer throughout its 25 year history. The weakly bound Ar–H_2S provided a dramatic example for the floppiness of van der Waals clusters showing an anomalous isotope effect. The rotational constants for Ar–H_2S turned out to be smaller than that of the heavier Ar–D_2S and, obviously, no rigid geometry could explain this observation.[108] de Oliveira and Dykstra[109] calculated vibrationally averaged rotational constants for the ground vibrational state using rigid body diffusion quantum Monte Carlo method for the two isotopomers and succeeded in rationalizing this experimental observation. Their detailed potential energy surface calculation showed a low energy trough with small energy barriers for the orbit of Ar about H_2S. Interestingly, similar calculations on Ne–H_2S predicted a relatively normal isotope effect.[110] Liu and Jäger reported the rotational spectra of Ne–H_2S and Ne–D_2S and the isotope effect was in reasonable agreement with Dykstra's predictions.[111]

Jäger's group has continued extensive studies on rare gas-molecule clusters identifying the first mixed rare gas-molecule trimer, $ArNeCO_2$.[112] They have also looked at several other rare gas and mixed rare gas clusters including Ar–N_2O, Ne–N_2O, ArNeHCl, Ar_2–N_2O, Ne_2–N_2O, Ne_2–OCS, Kr–H_2O, $ArNeN_2O$, Kr–NH_3, Ne–NH_3, Ar_3–NH_3, Ne_2–NH_3, and Ne_3–NH_3. More importantly, they have been able to observe several He containing clusters starting with He–CO.[113] Helium being the least polarizable of the rare gases, formation of He-molecule clusters is more difficult than other rare gas-molecule clusters. Recently, they have reported He_n–OCS, $n = 2–8$[114] and He_n–N_2O, $n = 3–12$[115] clusters and these are probably the largest clusters to be studied by high resolution spectroscopy. In the He_n–N_2O cluster series, the moments of inertia increase for $n = 3–6$ but shows oscillatory behavior for $n = 7–12$. The oscillatory behavior has been interpreted as evidence for decoupling of He atoms from N_2O in this size regime. It has also been taken as evidence for the transition from a molecular complex to a quantum solvated system, directly exploring the microscopic evolution of molecular superfluidity.

B. Molecular Clusters

Rotational spectra of molecular clusters offer a direct probe for determining the intermolecular potential energy surface. We restrict our discussion in this section to aromatic clusters and a series of interesting cylindrical

trimers such as $(OCS)_3$ reported by Kuczkowski et al.[116] and some N_2O clusters reported by Leung et al.

When it comes to aromatic interactions, benzene dimer is obviously the most important system for detailed investigations. However, there has been only a short communication[117] about the resolved rotational spectrum of "a benzene dimer." The sensitivity of the PNFTMW spectrometer played a crucial role in observing this spectrum which remained elusive. The spectra could be fit to a T-shaped structure and the intermolecular distance was estimated to be 4.96 Å, very close to that of solid benzene. This short communication remains the most direct structural determination of this important dimer. Internal rotation of either or both benzenes leads to a very complicated spectrum and only a small fraction of it has been assigned. The parallel-displaced structure of benzene dimer is theoretically predicted to be more stable than the T-shaped structure.[118] It is certainly more important when one looks at the staggering evidences for aromatic π stacking in condensed phase. However, it does not have a dipole moment and hence not amenable to investigations by PNFTMW spectrometer. Later in this review, we define an electrophore, which should prove useful for rotational spectroscopic studies on this interesting dimer. Recently, Stahl's group has reported the observation of 1,2-difluorobenzene dimer, which has a parallel, stacked structure.[119] Only c-dipole transitions were observed and each line was split by 110 kHz into two tunneling components. Ring planes were assumed to be parallel and the distance between them was estimated to be 3.45 Å. In the equilibrium structure, both rings are rotated by an angle of 130.3° against each other.

A detailed report on $C_6H_6-H_2S$ dimer has been published[120] along with comparison to results[121] on $C_6H_6-H_2O$, recently. Both of them have similar structure with H_2X lying along the C_6 axis resulting in a symmetric top spectrum for the ground state. However, several excited internal rotor/tunneling states have been observed for both these complexes and the spectra of these excited states have little in common for the two dimers. Experimental results on hydrogen bonded complexes with first and second group hydrides will be useful in bringing out the similarities and differences in bonding. Molecular mechanics in clusters calculations indicate that the intermolecular potential surface is more floppy for the H_2S complex compared to H_2O complex.[120] Rodham et al. have reported the observation of $C_6H_6-NH_3$ dimer, which appears to be the only gas phase complex (other than ammonia dimer) with NH_3 acting as a hydrogen bond donor.[122]

Rotational spectrum of fluorobenzene–HCl[123] and fluorobenzene–H_2O[124] have been determined quite recently. These two systems offer a study in contrast. The HCl complex had its geometry very similar to that of benzene–HCl complex, which was reported 20 years back.[125] Both C_6H_6–HCl and C_6H_5F–HCl complexes involve primarily π-hydrogen bonding.

However, such a π-hydrogen bonded minimum has not been observed for $C_6H_5F-H_2O$ complex. Initial searches for this complex assuming a structure similar to $C_6H_6-H_2O$ yielded no results. Ab initio calculations by Tarakeshwar et al.[126] on this system predicted that the $F\cdots HO$ σ-hydrogen bonded complex would be more stable than the π-hydrogen bonded complex. In addition to the $F\cdots HO$ interaction, theory predicted a $CH\cdots O$ hydrogen bonding interaction as well, leading to a 6-member ring formation involving HCCF of fluorobenzene and OH of H_2O. A search with rotational constants predicted from such a σ-hydrogen bonded structure was successful. The secondary $CH\cdots Cl$ interaction in C_6H_5F-HCl is likely to be weaker compared to that in the analogous H_2O complex. It would be interesting to look at C_6H_5F-HF dimer which should favor the σ-hydrogen bonded complex in preference to the π-hydrogen bonded complex.

Kuczkowski et al. have reported an interesting series of trimers involving nearly all permutations of OCS, CO_2, C_2H_2, C_2H_4, N_2O, and SO_2. Almost all these trimers have a barrel like structures with the three "linear" molecules forming three columns. In many cases, the dimer had to be investigated first for a detailed comparison of the structures. For example, after looking at several trimers in the series, before proceeding to trimers containing C_2H_4 and OCS, they characterized the C_2H_4-OCS dimer.[127] In the dimer, the OCS lies above the C_2H_4 plane, approximately parallel to the C═C. The $(C_2H_4)-(OCS)_2$ trimer was investigated later.[128] It had an equilibrium structure in which the plane of the ethylene is roughly parallel to the plane formed by the two OCS molecules. The two OCS monomers were aligned with parallel dipoles unlike what has been observed in the OCS dimer[129] or $(OCS)_2-CO_2$ trimer,[130] in which the two OCS monomers are aligned antiparallel. The $HCCH-(OCS)_2$ also had a similar structure to that of $(C_2H_4)-(OCS)_2$.[131] The study on $(CO_2)_2-N_2O$ draws our attention for two reasons. It is noted that the coaxial injection of molecular beam resulted in lowering of intensity compared to the original perpendicular orientation, unlike in all other laboratories. This highlights the fact that the PNFTMW spectrometers are home-made and each one of the 25 plus spectrometers may be unique. In addition, the authors have pointed out that the rotational constants for the parent isotopomer and the dipole moment of the trimer could not distinguish between $(CO_2)_2-N_2O$ and $(CO_2)-(N_2O)_2$. Getting the spectrum for $(^{13}CO_2)_2-N_2O$ helped in resolving the ambiguity and proved the complex to be $(CO_2)_2-N_2O$.

Leung et al. have been systematically investigating a series of N_2O complexes to explore the nature of bonding through the quadrupole coupling constants for the two N nuclei present in the system. Their main objective is to test the assumption frequently made in the analysis of quadrupole coupling constants in weakly bound complexes. It is generally assumed that the

change observed in quadrupole coupling constants for an atom in the monomer and in the complex is attributable to the orientation of the monomer in the complex. By comparing the two values, the projection angle is determined. Having two ^{14}N quadrupolar nuclei in N_2O implies that quadrupole coupling constants for both should lead to the same projection angle, if this assumption is valid. They have observed that for only one ($OCS-N_2O$) out of five ($Ar-N_2O$, $HCCH-N_2O$, CO_2-N_2O, and N_2-N_2O being the other four), this assumption is valid. Recently, they have reinvestigated the linear and bent isomers of $HF-N_2O$ complex[132] and looked at $HF-{}^{15}N^{14}NO$, $HF-{}^{14}N^{15}NO$, and $HF-{}^{15}N_2O$ isotopomers. As ^{15}N does not have a quadrupole moment, the rotational spectrum of $HF-{}^{15}N_2O$ has been used to determine the HF spin–spin coupling constant. The rotational spectra of the other two isotopomers have yielded the ^{14}N quadrupole coupling constants for both the terminal and the central N. These results have been used to deduce that in the linear isomer, electric field gradient of N is perturbed on hydrogen bond formation but such a perturbation is not found in the bent isomer.

C. Molecular Conformers, Chiral Molecules and Their Complexes

Though, weakly bound complexes have been attracting a lot of attention, the sensitivity and resolution of PNFTMW spectrometer has been simultaneously exploited for looking at rotational spectra of several interesting monomers recently. Many of them have numerous conformers and are of biological interest. To highlight advances in this direction, a few examples are discussed in this section.

Fraser et al. have reported PNFTMW investigations on 1-pentene,[133] 1-hexene,[134] and 1-octene[135] in recent years. These simple unbranched hydrocarbon chains are rich in the number of conformational isomers. According to ab initio and molecular modeling 1-pentene, 1-hexene, and 1-octene are expected to have 5, 13, and 131 conformational isomers, respectively. Out of these, PNFTMW spectrometer has provided the rotational spectrum of 4, 7, and 15 conformational isomers, respectively. For 1-octene, the 15 conformers observed are within an energy spread of $365\,cm^{-1}$ according to molecular mechanics calculations. Fourteen of the 15 conformers observed are positively assigned to 14 of the 15 lowest energy minima predicted. Conformational cooling is not very efficient in supersonic expansion and this facilitates the observation of many of the conformers that are present in the room temperature sample. The advances in automatic scanning of the PNFTMW spectrometer at NIST have vastly benefited this effort. The low resolution survey spectrum of 1-octene is

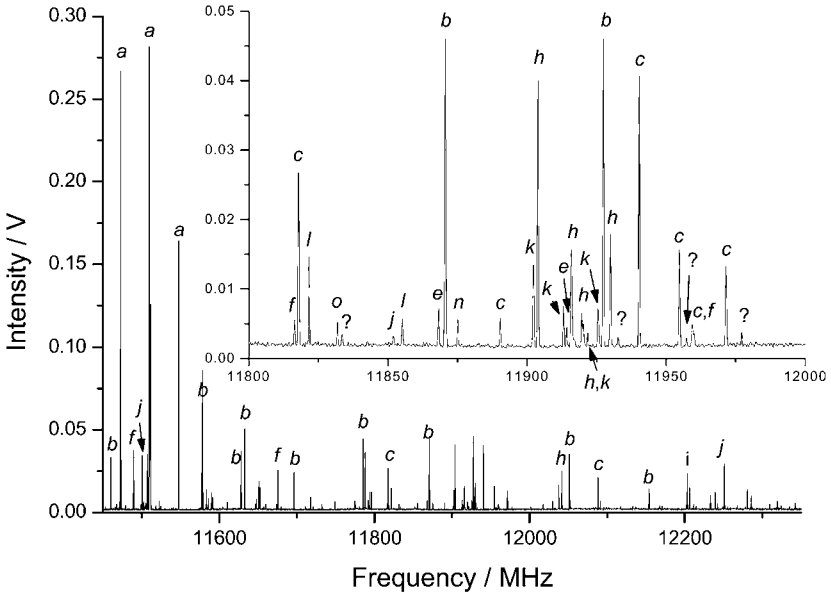

Figure 10. Part of the survey spectrum for 1-octene taken from 11.4 to 12.4 GHz. The lines are labeled a–o to identify the 15 different conformers. Inset shows an expanded view of 200 MHz spectrum. *Source:* See Ref.[135] for details. Reproduced with permission from American Chemical Society.

shown in Fig. 10. The 1-GHz spectrum shown is the result of 2000 or 4000 experiments with 500 or 250 kHz step size. The fact that this could be done in about an hour would be greatly appreciated by many of the practitioners in the field who have spent days to collect such information (see also Fig. 1 of Ref.[82] showing a 3 GHz spread spectrum of HfO and HfO_2). These results should prove important for theoretical investigations to test the hydrocarbon force field.

Tuberjen et al. have been investigating the rotational spectra of several amino acids, derivatives, and their complexes. They have reported the rotational spectra of amino acid derivatives like alaninamide,[136] prolinamide,[137] and valinamide.[138] These structures have intramolecular hydrogen bonds from the amide to amine groups and similar in structure to the higher energy amino acid conformer. Similarly *N*-acetyl-alanine *N*′-methylamide (AAMA) is a model for protein conformation study as it contains two peptide bonds. Lavrich et al.[139] have taken a different approach for conformational identification for this molecule other than isotopic substitution. AAMA has three methyl groups, two of which have low V_3 barrier and cause

torsion–rotation splitting in microwave spectrum. Analysis of these spectra enabled them to get two different sets of angles to define the three dimensional orientation of these methyl groups. These angles proved to be unique for a particular conformer.

Alonso et al. have been looking at conformational isomers in hydrogen bonded complexes. For example, they have studied the axial and equatorial hydrogen bonded pentamethylene sulfide–HCl/HF,[140,141] tetrahydropyran–HCl/HF,[142,143] and trimethylene sulfide–HF complexes.[144] The structures of axial and equatorial trimethylene sulfide–HF complexes are shown in Fig. 11. The axial conformer has been found to be the most stable. It has been possible to observe the conformational relaxation of the equatorial form to axial form by varying the carrier gas from He to Ar. Ruoff et al. have earlier shown that the conformational relaxation would be complete in supersonic expansion with Ar, if the barrier is less than $400\,cm^{-1}$ [145] and only the low energy conformers would be present. Interestingly, for pentamethylene sulfide–HX complex, the barrier for conversion is much larger, $4057\,cm^{-1}$,[146] and both axial and equatorial hydrogen bonded complexes could be observed in Ar. Alonso et al. have also reported the construction of a laser ablation source especially for studying organic and biomolecules recently.[147] This has been used to record the spectrum of the neutral proline.[148]

Alonso et al. have used the PNFTMW spectrometer for recording the first gas phase complex containing C–H···O hydrogen bonds,[149] as well. The complex is the dimer of dimethyl ether. Experimental rotational constants of six isotopomers have been used to determine the structure in terms of $R_{c.m.}$, θ_1, and θ_2, where $R_{c.m.}$ is the distance between the c.m. of the two monomers, θ_1 and θ_2 are the angle between the line connecting the c.m. and the C_{2v} axis of monomers 1 and 2. The structure of a monomer had been fixed in doing this estimation. The experimental rotational constants is in reasonable agreement with a structure involving 3 C–H···O hydrogen bonds, as shown in Fig. 12. Theoretical calculations have indicated that there is a shortening of C–H bond in the dimer compared to the monomer leading the authors to characterize this interaction as improper, blue shifting hydrogen bond. As the decrease in C–H bond length is rather small, experimental evidence from rotational spectroscopy for such a decrease would be very difficult to establish. However, experimental evidence for blue shifting in C–H stretching frequency has been obtained by Hobza and coworkers[150] using infrared spectra of 1 : 1 complex of dimethyl ether and fluoroform in liquid Ar. For a theoretical explanation on the reasons for blue-shifting hydrogen bonds, the reader is referred to an interesting article by Hermansson.[151]

Howard et al. have been interested in observing intermolecular complexes of chiral molecules, with the objective of understanding enantiospecificity in biological and pharmaceutical compounds. Enzyme and substrate are both

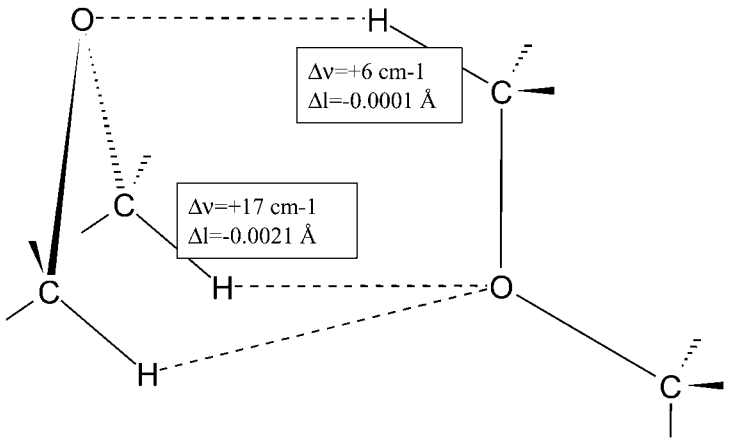

Figure 11. Structures of axial and equatorial conformers of trimethylene sulfide $\cdots$HF. *Source:* Reproduced with permission from Wiley-VCH, Ref.[144].

chiral and their interaction can be probed by studying van der Waals complexes between two chiral species. The van der Waals complex formed between two chiral species can have *R*–*R*, *S*–*S*, *R*–*S*, and *S*–*R* conformations in the complex. The *R*–*R* and *S*–*S* complexes are called homochiral and they will be enantiomers. Similarly, the heterochiral *R*–*S* and *S*–*R* complexes will be enantiomers. With this objective in mind, King and Howard investigated 2-butanol with PNFTMW spectrometer and identified three of the nine possible conformers arising from the C–C and C–O single bond rotations.[152] Three conformers in supersonic expansion imply potentially nine different forms of the dimer. The two lone pairs on oxygen atom are not equivalent and it could lead to two different complexes as discussed in the last paragraph. King and Howard have identified the rotational spectrum of *R*2*S* heterochiral dimer, where the 2 identifies the lone pair involved in hydrogen bonding.[153] Howard's group has also been looking at open shell complexes such as Kr–NO_2.[154] A Helmholtz coil is used to compensate the earth's magnetic field to remove the Zeeman splitting observed.

IV. HYDROGEN BOND RADII AND ELECTROPHORE

In Section II and III, all the advances and direct applications of PNFTMW spectrometer have been discussed. In this section, we introduce some concepts that evolve as a result of the vast structural data that have become available in the past two decades.

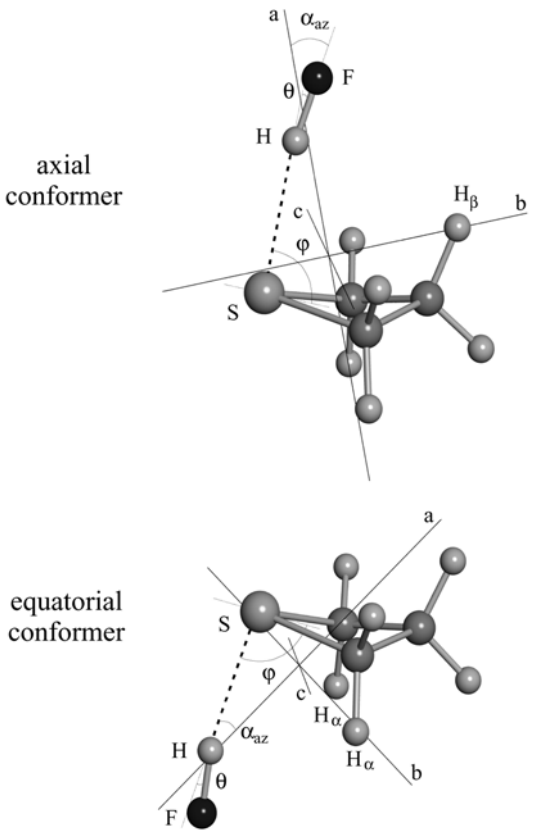

Figure 12. Shortening of the C–H bond lengths and blue shift of the corresponding stretching vibrations, upon formation of the dimer, of the C–H groups involved in the H bond, based on ab initio investigations. Microwave spectrum does not give any evidence for this shortening as the change in distance is too small. However, IR spectroscopic evidence for the blue shift is available. See text for details. *Source:* Reproduced with permission from American Chemical Society, Ref.[149].

A. Hydrogen Bond Radius

Recently, by analyzing the accurate intermolecular distances for hydrogen bonded complexes, almost all of them determined by PNFTMW spectrometer, Mandal and Arunan defined a hydrogen bond radius for HF, HCl, HCN, and HBr[155] in B $\cdots$ HX complexes, where B is a hydrogen bond

acceptor. Gadre et al. have determined the electrostatic potentials for various B molecules and identified the location of global minimum.[156] They argued that these minima symbolize the sites of electron localization in molecules and act as probable proton attractors. The distance from the bonding center in B, which may be an atom or center of a π electron cloud to the electrostatic minimum, R_{esp} was close to the van der Waals radius of the atom in B. They noted that for several B $\cdots$ HF complexes, the B–H distance was the sum of R_{esp} and a constant, 0.47 Å. Mandal and Arunan extended this analysis to the other HX complexes and noted that this constant increased with decreasing dipole moment of HX. This constant was defined as hydrogen bond radius for the HX. An empirical linear correlation was found and it was pointed out that the intercept at zero dipole moment, 1.01 Å, was closer to the van der Waals radius of hydrogen atom, 1.2 Å. There appears to be no theoretical reasons for this linear correlation. Later on, this analysis was extended to HCCH and H_2O complexes as models for C–H and O–H hydrogen bonding.[40] Figure 13 shows the hydrogen bond radius for various hydrogen bond donors as a function of dipole moment of HX. The hydrogen bond radius in Fig. 13 has been extrapolated to 1.1 Å at zero dipole moment for HCCH in addition to the linear correlation. All the hydrogen bond radii determined from this analysis fall in between the covalent radius and van der Waals radius of hydrogen atom. Figure 13 offers yet another evidence that molecular interactions are continuous from the strong covalent to the weak van der Waals. A preliminary analysis of O–H–O, N–H–O, and C–H–O distances from the Cambridge crystal data base gives results in close agreement with Fig. 13.[157]

Recently, a similar analysis on ClF and Cl_2 complexes has shown that, Cl radius on these complexes follow a similar trend and fall in between the covalent and van der Waals radii of Cl.[158] Here again, most of the experimental data have come from PNFTMW spectrometer.

B. An Electrophore

Microwave spectroscopy is certainly limited in its applications. Only molecules that have a finite vapor pressure and a non-zero permanent dipole moment can be investigated. However, the information that can be obtained from microwave spectroscopy is often the most accurate and precise. Experimental advances such as pulsed discharge nozzle and laser ablation have certainly expanded the range of chemical systems that can be studied. Also, the sensitivity of FTMW spectrometers has allowed the observation of non-polar molecules under some conditions. Centrifugally induced pure rotational spectrum has been observed for the non-polar SO_3 molecule with

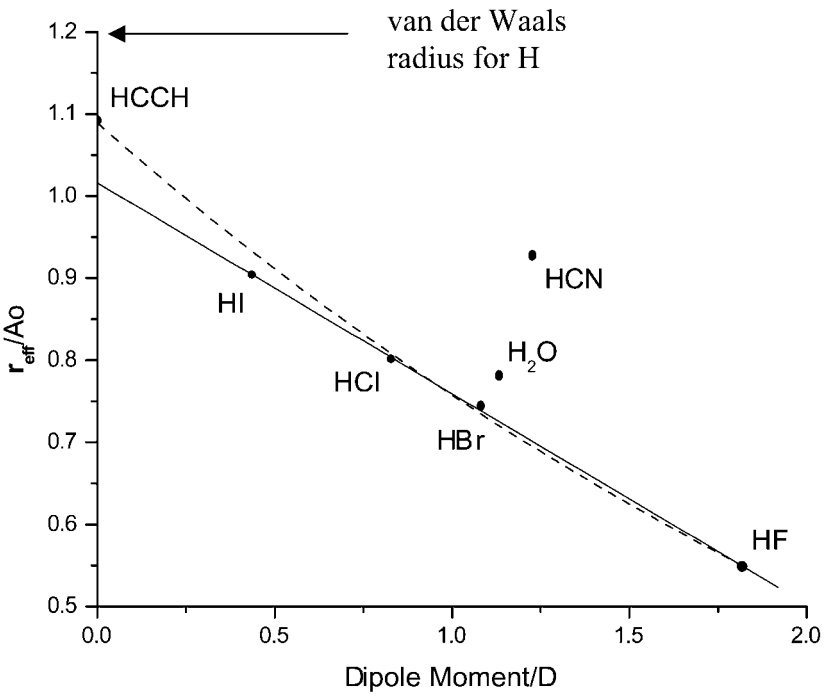

Figure 13. Hydrogen bond radius for various hydrogen bond donors as a function of dipole moment. Note that all these radii are between the covalent and van der Waals radii of hydrogen atom.

FTMW spectrometer.[159] Isotopically substituted molecules that have tiny dipole moments such as C_6H_5D[160] have been investigated as well. The difference in zero point oscillations between C–H and C–D groups generates a dipole in C_6H_5D. However, for $^{13}CC_5H_6$, the dipole moment would be much smaller if at all non zero and, so far, there have been no reports on its rotational spectrum. Here, we introduce the concept of an electrophore that can be used for getting the rotational spectrum of non-polar molecules, somewhat like a chromophore that gives color to a molecule. Table 5 lists the rotational constants for C_6H_5D and $^{13}CC_5H_6$ determined by the microwave investigations of C_6H_6–H_2O isotopomers, in which H_2O may be considered an electrophore. In this complex, the ground state has practically spherical H_2O and it does not contribute to the moments of inertia along the *a* inertial axis. Thus, the *A* rotational constant determined for the complex is virtually identical to the *C* rotational constant for the substituted benzene. The concept of an electrophore was used without recognition in studies on Ne–C_6H_6

Table 5. Rotational constants (in MHz) A for $C_6H_5D/{}^{13}CC_5H_6$–HX and C for $C_6H_5D/{}^{13}CC_5H_6$.

C_6H_5D		$^{13}CC_5H_6$	
HX	A/C	HX	A/C
—	2,749.674[a]	—	2,813[c]
H_2O	2,765.5(2)[b]	D_2O	2,832(4)[b]
D_2O	2,765.5(3)[b]	HCN	2,823(7)[d]
—	—	H_2S	2,837(6)[e]

[a]Ref.[160].
[b]Ref.[121]. The A rotational constant reported is incorrect for $^{13}CC_5H_6$–H_2O due to wrong assignment.
[c]No experimental results available, calculated from a rigid structure.
[d]Ref.[163].
[e]Ref.[120].

dimer. Initial attempts to obtain the rotational spectrum of this complex were unsuccessful.[161] Somewhat serendipitously, Arunan et al. observed the rotational spectrum of the sandwich trimer Ne–C_6H_6–H_2O[162] which provided a further impetus for a successful search of Ne–C_6H_6.[43] It turned out that the Ne–c.m.C_6H_6 distances were practically identical in Ne–C_6H_6 and Ne–C_6H_6–H_2O.

Table 6 lists the rotational constants for Ar_2 determined from electronic spectra as well as from the rotational spectra of the various Ar_2–X complexes.

Table 6. Rotational constants for Ar_2–HX (A or B).

X	B (MHz)	Reference
—	1,731.601	—[a]
Ne	1,739.717	[106]
HF	1,739.139	[164]
HCl	1,733.857	[165]
HBr	1,731.959	[166]
H_2O	1,734.651	[167]
HCN	1,743.854	[169]
H_2S	1,733.098	[168]

[a]Herman, P. R.; LaRoucque, P. E.; Stoicheff, B. P. J. Chem. Phys. **1988**, *89*, 4535. In all these complexes, X does not contribute to the moments of inertia about the principle axis bisecting Ar_2. The Ar–Ar distance varies by less than 0.01 Å in all the complexes.

As is evident, even Ne can be an electrophore for experimental determination of Ar–Ar distance in Ar_2 through rotational spectroscopy. The sensitivity and resolution of PNFTMW spectrometer were crucial in these experiments.

The concept of an electrophore can be useful in looking at tunneling states of various hydrogen bonded dimers. This became obvious during the detailed investigations on Ar–$(H_2O)_2$.[170] The $(H_2O)_2$ undergoes complicated tunneling motions leading to 8 isoenergetic minima that are labeled as A_1, B_1, E_1, A_2, B_2, and E_2.[171] It has strong *a* dipole component which is inverted following donor–acceptor interchange tunneling. The result is that only E states have rigid rotor spectrum and A and B states have tunneling spectra. Forming Ar–$(H_2O)_2$, introduced a dipole moment along the *b* axis of $(H_2O)_2$ (*a* axis for trimer), which remains unchanged during donor–acceptor interchange tunneling. Hence, for Ar–$(H_2O)_2$, all *a* dipole transitions were pure rotational transitions for A, B, and E states, though only E state has *b* dipole pure rotational transitions. Not surprisingly, the *A* rotational constant for Ar–$(H_2O)_2$ was very close to the *B* rotational constant for the $(H_2O)_2$.

Recently, Kisiel et al. have studied $(H_2O)_2$–HCl[172] and $(H_2O)_2$–HBr.[173] They pointed out the importance of studying water multimers, $(H_2O)_n$ and noted that the first in such series, $(H_2O)_3$, has no dipole moment. By changing one of the (H_2O) to HX, two non-zero dipole moment components have been introduced. Clearly, the concept of an electrophore has been used. The *A* rotational constant for Ar–$(H_2O)_2$, HBr–$(H_2O)_2$, and HCl–$(H_2O)_2$ are 6253, 6770, and 6875 MHz compared to the *B* of 6160.7 MHz for $(H_2O)_2$.[65] As the *a* axis for the trimer is practically the *b* for dimer, it points to a reduction in O–O distance of 0.035, 0.153, and 0.155 Å in Ar–$(H_2O)_2$, HBr–$(H_2O)_2$, and HCl–$(H_2O)_2$, respectively compared to $(H_2O)_2$. As is evident, forming the trimer with HCl and HBr alters the $(H_2O)_2$ quite significantly. Moreover, the tunneling dynamics of $(H_2O)_2$ is altered as well, with four closely spaced (<1 MHz spacing) tunneling states observed for HBr–$(H_2O)_2$ and HCl–$(H_2O)_2$, with no obvious similarity to the $(H_2O)_2$ tunneling states. Even in the Ar–$(H_2O)_2$ trimer, the tunneling splitting is significantly reduced. It was found to be 106 MHz for Ar–$(D_2O)_2$ compared to 1 GHz for $(D_2O)_2$. Information of $(H_2O)_3$ could be more directly observed by a detailed look at Ar–$(H_2O)_3$. Preliminary results on Ar–$(H_2O)_3$[174] showed qualitatively similar tunneling states as observed in the far-IR spectrum of $(H_2O)_3$.[175] For $(H_2O)_3$, a symmetric quartet with a spacing of 289 MHz was observed but in Ar–$(H_2O)_3$ this splitting reduced to about 40 kHz.

The tunneling frequencies are often in mm or far IR region, making it difficult for observation with PNFTMW spectrometer. All the $(HX)_2$ exhibit such tunneling and except for $(HF)_2$, no transitions could be observed in microwave

region for $(HCl)_2$ and $(HBr)_2$. Novick et al. overcame this problem by isotopic substitution to quench the tunneling and obtained the rotational spectrum for HBr–DBr.[176] Howard et al. had earlier observed microwave transitions for HCl–DCl.[177] Rotational spectrum of $Ar–(HCl)_2$ and $Ar–(HBr)_2$ could provide detailed information about the HX dimer as well as the trimer. As of now, there appears to be no report on $Ar–(HX)_2$ for any hydrogen halides, though there have been several attempts[178] to look for $Ar–(HF)_2$.

We note that the investigations of Fraser et al. on a series of 1-alkenes[133–135] have been stimulated by the same concept. As a means to study the conformations of *n*-alkanes that have zero or tiny dipole moments, they have utilized the polar end group in alkenes.

V. CONCLUSIONS

It is 25 years now, since Balle and Flygare developed the PNFTMW spectrometer. In their first article describing the spectrometer,[6] they had anticipated the use of a high temperature nozzle for looking at heavy molecules with low vapor pressure and rare gas-metal atom dimers. They had suggested that "by crossing the nozzle expansion with some excitation source such as a laser, electron beam, or plasma, one might be able to see rotational transitions in excited states." They also observed that other types of nozzle sources might allow one to observe combustion or explosion products. Finally, they had hoped that molecular radicals and ions would be studied using this technique. Electron beam and plasma are yet to be used along with the PNFTMW spectrometer, to the best of our knowledge. However, this review clearly points out that the practitioners in this field from all over the world have achieved everything Flygare had hoped and a whole lot more using this spectrometer. Klemperer observed that the supersonic expansion technique has reduced the synthesis of weakly bound complexes to a two-step process: buy the components and expand.[179] The high temperature nozzle, coaxial mixing nozzle, and laser ablation sources have made it possible to study virtually any chemical species or complex by rotational spectroscopy, even the ones that cannot be bought or the ones that would prefer to react, rather than forming a weakly bound complex! The fact that several new spectrometers have been fabricated in the last few years suggests that the horizons of applications of PNFTMW spectrometer will be widening further. Just after the completion of this review, we have learned about the arrival of yet another PNFTMW spectrometer.[180]

ACKNOWLEDGMENTS

All the FTMW groups are acknowledged for providing (p)reprints of their work which made the task simpler. Work at the author's laboratory is supported by a generous grant from the Department of Science and Technology, India and the Director, Indian Institute of Science. Dharmender Ramdass helped in artwork. E.A. is indebted to his former collaborators Tryggvi Emilsson and late Prof. H. S. Gutowsky who introduced him to the PNFTMW spectrometer and Prof. C. E. Dykstra for stimulating discussions on intermolecular interactions.

REFERENCES

1. Townes, C.H.; Schawlow, A.L. *Microwave Spectroscopy*; McGraw-Hill: New York, 1955; Dover, New York, 1975.
2. Sugden, T.M.; Kenney, C.N. *Microwave Spectroscopy of Gases*; D. van Nostrand: New York, 1965.
3. Wollrab, J.E. *Rotational Spectra and Molecular Structure*; Academic Press: New York, 1967.
4. Kroto, H.W. *Molecular Rotation Spectra*; Wiley (Interscience): New York, 1975.
5. Gordy, W.; Cook, R. *Microwave Molecular Spectra,* II Ed.; John Wiley & Sons: New York, 1984.
6. Balle, T.J.; Flygare, W.H. Fabry–Perot cavity pulsed Fourier transform microwave spectrometer with a pulsed nozzle particle source. Rev. Sci. Instrum. **1981**, *52* (1), 33–45.
7. Novick, S.E.; Janda, K.C.; Holmgren, S.L.; Waldman, M.; Klemperer, W. Centrifugal distortion in argon hydrogen chloride (ArHCl). J. Chem. Phys. **1976**, *65* (3), 1114–1116.
8. Balle, T.J.; Campbell, E.J.; Keenan, M.R.; Flygare, W.H. A new method for observing the rotational spectra of weak molecular complexes: KrHCl. J. Chem. Phys. **1979**, *71* (6), 2723–2724 and **1980**, *72* (2), 922–932.
9. Legon, A.C. Pulsed-nozzle, Fourier-transform microwave spectroscopy of weakly bound dimers. Annu. Rev. Phys. Chem. **1983**, *35*, 275–300.
10. Legon, A.C. Fourier transform microwave spectroscopy. In *Atomic and Molecular Beam Methods*; Scoles, G., Ed.; Oxford University Press: New York, 1992; Vol. 2, 192–210.
11. Bettens, F.L.; Bettens, R.P.A.; Bauder, A. Rotational spectroscopy of weakly bound complexes. In *Jet Spectroscopy and Molecular Dynamics*;

Hollas, J.M., Phillips, D., Eds.; Kluwer Academic Publishers: Dordrecht, 1995; 1–28.

12. Dreizler, H. Fourier transform microwave spectroscopy—an improved tool for investigation of rotational spectra. Ber. Bunsenges. Phys. Chem. **1995**, *99* (12), 1451–1461.
13. Suenram, R.D.; Andrews, A.M. Microwave spectroscopy. In *Experimental Methods in Physical Sciences*; Dunning, F.B., Hulet, R.G., Eds.; Academic Press: 1996; Vol. 29B, 273–299.
14. Leopold, K.R.; Fraser, G.T.; Novick, S.E.; Klemperer, W. Current themes in microwave and infrared spectroscopy of weakly bound complexes. Chem. Rev. **1994**, *94* (7), 1807–1827.
15. Legon, A.C. Pre-reactive complexes of dihalogens XY with Lewis bases B in the gas phase: a systematic case for the "halogen" analogue B···XY of the hydrogen bond B···HX. Angew. Chem. Int. Ed. Engl. **1999**, *38* (18), 2686–2714.
16. Novick, S.E. Bibliography of Rotational Spectra of Weakly Bound Complexes, 2003; http://www.wesleyan.edu/chem/faculty/novick/vdw.html.
17. Kisiel, Z. Rotational Spectroscopy Links, 2003; http://info.ifpan.edu.pl/~kisiel/rotlinks.htm.
18. Lovas, F.J.; Suenram, R.D. Pulsed beam Fourier transform microwave measurements on OCS and rare gas complexes of OCS with Ne, Ar, and Kr. J. Chem. Phys. **1987**, *87* (4), 2010–2020.
19. Lida, M.; Ohshima, Y.; Endo, Y. Rotational spectra, structure, and intermolecular force field of the Hg–OCS van der Waals Complex. J. Chem. Phys. **1991**, *94* (11), 6989–6994.
20. Bumgarner, R.E.; Kukolich, S.G. Microwave spectra and structure of HI-HF complexes. J. Chem. Phys. **1987**, *86* (3), 1083–1089.
21. Hillig, K.W. II.; Matos, J.; Scioly, A.; Kuczkowski, R.L. The microwave spectrum of argon–phosphorous trifluoride. Chem. Phys. Lett. **1987**, *133* (4), 359–362.
22. Xu, Y.; Jäger, W.; Gerry, M.C.L. The rotational spectrum of the isotopically substituted van der Waals complex ArOCS, obtained using a pulsed beam microwave Fourier transform spectrometer. J. Mol. Spectrosc. **1992**, *151* (1), 206–216.
23. Brupbacher, Th.; Bauder, A. Rotational spectrum and dipole moment of the benzene–argon van der Waals complex. Chem. Phys. Lett. **1990**, *173* (5–6), 435–438.
24. Suenram, R.D.; Lovas, F.J.; Fraser, G.T.; Gillies, J.Z.; Gillies, C.W.; Onda, M. Microwave spectrum, structure, and electric dipole moment of argon–methanol. J. Mol. Spectrosc. **1989**, *137* (1), 127–137.

25. Krüger, M.; Dreizler, H. A microwave Fourier transform spectrometer with a single microwave source. Z. Naturforsch. **1990**, *45a*, 724–726.
26. Grabow, J.-U.; Stahl, W. A pulsed beam microwave Fourier transform spectrometer with parallel molecular beam and resonator axes. Z. Naturforsch. **1990**, *45a*, 1043–1044.
27. Chuang, C.; Hawley, C.J.; Emilsson, T.; Gutowsky, H.S. Computer-based controller and averager for the Balle–Flygare spectrometer. Rev. Sci. Instrum. **1990**, *61* (6), 1629–1635.
28. Andresen, U.; Dreizler, H.; Grabow, J.-U.; Stahl, W. An automatic molecular beam microwave Fourier transform spectrometer. Rev. Sci. Instrum. **1990**, *61* (12), 3694–3699.
29. Grabow, J.-U.; Stahl, W.; Dreizler, H. A multioctave coaxially oriented beam resonator arrangement Fourier transform microwave spectrometer. Rev. Sci. Instrum. **1996**, *67* (12), 4072–4084.
30. Low, R.J.; Varberg, T.D.; Connelly, J.P.; Auty, A.R.; Howard, B.J.; Brown, J.M. The hyperfine structures of CuCl and CuBr in their ground states studied by microwave Fourier transform spectroscopy. J. Mol. Spectrosc. **1993**, *161* (2), 499–510.
31. Hight Walker, A.R.; Chen, W.; Novick, S.E.; Bean, B.D.; Marshall, M.D. Determination of the structure of HBr–OCS. J. Chem. Phys. **1995**, *102* (19), 7298–7305.
32. Warner, H.E.; Wang, Y.; Ward, C.; Gillies, C.W.; Interrante, L. Microwave study of the CVD precursor trimethylamine–alane, $(CH_3)_3N–AlH_3$: rotational spectra, ^{27}Al and ^{14}N nuclear quadrupole coupling constants, and molecular structure. J. Phys. Chem. **1994**, *98* (47), 12215–12222.
33. Alonso, J.L.; Lorenzo, F.J.; López, J.C.; Lesarri, A.; Mata, S.; Dreizler, H. Construction of a molecular beam Fourier transform microwave spectrometer used to study the 2,5-dihydrofuran–argon van der Waals complex. Chem. Phys. **1997**, *218* (3), 267–275.
34. Harmony, M.D.; Beran, K.A.; Angst, D.M.; Ratzlaff, K.L. A compact hot-nozzle Fourier-transform microwave spectrometer. Rev. Sci. Instrum. **1995**, *66* (11), 5196–5202.
35. Phillips, J.A.; Canagaratna, M.; Goodfriend, H.; Grushow, A.; Almolöf, J.; Leopold, K.R. Microwave and ab initio investigation of $HF–BF_3$. J. Am. Chem. Soc. **1995**, *117* (50), 12549–12556.
36. Xu, Y.; Jäger, W. Evidence for heavy atom large amplitude motions in RG-cyclopropane van der Waals complexes (RG = Ne, Ar, Kr) from rotation-tunneling spectroscopy. J. Chem. Phys. **1997**, *106* (19), 7968–7980.
37. Tuberjen, M.J.; Flad, J.E.; Del Bene, J.E. Microwave spectroscopic and ab initio studies of the hydrogen-bonded trimethylamine–hydrogen sulfide complex. J. Chem. Phys. **1997**, *107* (7), 2227–2231.

38. Leung, H.O. The microwave spectrum and nuclear quadrupole hyperfine structure of HCCH–N_2O. J. Chem. Phys. **1997**, *107* (7), 2232–2241.
39. Kisiel, Z.; Kosarzewski, J.; Pszczolkówski, L. Nuclear quadrupole coupling tensor of CH_2Cl_2: comparison of quadrupolar and structural angles in methylene halides. Acta Physical Polanica A **1997**, *92* (2), 507–516.
40. Arunan, E.; Tiwari, A.P.; Mandal, P.K.; Mathias, P.C. Pulsed nozzle Fourier transform microwave spectrometer: ideal to define hydrogen bond radius. Curr. Sci. **2002**, *82* (5), 533–540.
41. Storm, V.; Dreizler, H.; Consalvo, D.; Grabow, J.-U.; Merke, I. A newly designed molecular beam Fourier transform microwave spectrometer in the range 1–4 GHz. Rev. Sci. Instrum. **1996**, *67* (8), 2714–2719.
42. Merke, I.; Stahl, W.; Dreizler, H. A molecular beam Fourier transform microwave spectrometer in the range 26.5 to 40 GHz. Tests of performance and analysis of the D- and ^{14}N-hyperfine structure of methylcyanide-d. Z. Naturforsch. **1994**, *49a*, 490–496.
43. Arunan, E.; Emilsson, T.; Gutowsky, H.S. Rotational spectra and structures of Rg–C_6H_6–H_2O trimers and Ne–C_6H_6 dimer (Rg = Ne, Ar, or Kr). J. Chem. Phys. **1994**, *101* (2), 861–868.
44. Suenram, R.D.; Grabow, J.-U.; Zuban, A.; Leonov, I.A. Portable pulsed-molecular-beam Fourier-transform microwave spectrometer designed for chemical analysis. Rev. Sci. Instrum. **1999**, *70* (4), 2127–2135.
45. Andreson, U.; Dreizler, H.; Kretschmer, U.; Stahl, W.; Thomsen, C. A molecular beam Fourier transform microwave spectrometer developed for analytical purposes. Fresenius J. Anal. Chem. **1994**, *349*, 272–276.
46. Shea, J.A.; Campbell, E.J. The rotational spectra, molecular structures, and mercury-201 nuclear quadrupole coupling constants of mercury hydrogen chloride (HgHCl) and mercury deuterium chloride (HgDCl). J. Chem. Phys. **1984**, *81* (12), 5326–5235.
47. Lida, M.; Ohshima, Y.; Endo, Y. Rotational spectra, structure, and intermolecular force field of the Hg–OCS van der Waals Complex. J. Chem. Phys. **1991**, *94* (11), 6989–6994.
48. Gutowsky, H.S.; Chen, J.; Hajduk, P.J.; Keen, J.D.; Chuang, C.; Emilsson, T. Silicon–carbon double bond: theory takes a round. J. Am. Chem. Soc. **1991**, *113* (13), 4748–4751.
49. Arunan, E.; Emilsson, T.; Gutowsky, H.S. Excited ν_3 vibrational state of the Ar–HCN and Kr–HCN dimers. J. Chem. Phys. **1995**, *103* (2), 493–496.
50. Legon, A.C.; Stephenson, D. Microwave spectroscopy of pyrolytically produced, rapidly isolated transient molecules. J. Chem. Soc. Faraday Trans. **1991**, *87* (19), 3325–3326.

51. Kukolich, S.G.; Sickafoose, S.M.; Breckendridge, S.M. Microwave molecular structure measurements for tetracarbonyldihydroosmium, a classical dihydride. J. Am. Chem. Soc. **1996**, *118* (1), 205–208.
52. Drouin, B.J.; Kukolich, S.G. Molecular structure of tetracarbonyldihydroiron: microwave measurements and density functional calculations. J. Am. Chem. Soc. **1998**, *120* (27), 6774–6780.
53. Drouin, B.J.; Greg Levaty, T.; Cassak, P.A.; Kukolich, S.G. Measurements of structural and quadrupole coupling parameters for bromoferrocene using microwave spectroscopy. J. Chem. Phys. **1997**, *107* (17), 6541–6548.
54. Suenram, R.D.; Lovas, F.J.; Pluquellic, D.F.; Lesarri, A.; Kawashima, Y.; Jensen, J.O.; Samuels, A.C. Fourier transform microwave spectrum and ab initio study of dimethyl methylphosphonate. J. Mol. Spectrosc. **2002**, *211* (1), 110–118.
55. Emilsson, T.; Klots, T.D.; Ruoff, R.S.; Gutowsky, H.S. Rotational spectra and structures of the OC- and H_3N–HCN–HF mixtures: coaxial mixing nozzle for reactive species. J. Chem. Phys. **1990**, *93* (10), 6971–6976.
56. Legon, A.C.; Rego, C.A. Rotational spectrum of $(CH_3)_3P\cdots HCl$ and a comparison of properties within a series of axially symmetric dimers $R_3Y\cdots HCl$, where Y = N or P and R = H or CH_3. J. Chem. Soc. Faraday Trans. **1990**, *86* (11), 1915–1921.
57. Legon, A.C.; Wallwork, A.L.; Rego, C.A. The rotational spectrum and nature of the heterodimer in trimethylammonium bromide vapor. J. Chem. Phys. **1990**, *92* (11), 6397–6407.
58. Legon, A.C.; Campbell, E.J.; Flygare, W.H. The rotational spectrum and molecular properties of a hydrogen-bonded complex formed between hydrogen cyanide and hydrogen chloride. J. Chem. Phys. **1982**, *76* (5), 2267–2274.
59. Howard, N.W.; Legon, A.C. Nature, geometry and binding strength of the ammonia–hydrogen chloride dimer determined from the rotational spectrum of ammonium chloride vapor. J. Chem. Phys. **1988**, *88* (8), 4694–4701.
60. Legon, A.C.; Rego, C.A. Microwave spectrum, structure and internal rotation of the methylamine–hydrogen chloride dimer. J. Chem. Soc. Faraday Trans. **1993**, *89* (8), 1173–1178.
61. Legon, A.C.; Rego, C.A. An investigation of the trimethylammonium chloride molecule in the vapor phase by pulsed-nozzle, Fourier-transform microwave spectroscopy. J. Chem. Phys. **1989**, *90* (12), 6867–6876.
62. Phillips, J.A.; Canagaratna, M.; Goodfriend, H.; Leopold, K.R. Microwave detection of a key intermediate in the formation of atmospheric

sulfuric acid: the structure of H_2O-SO_3. J. Phys. Chem. **1995**, *99* (2), 501–504.

63. Fiacco, D.L.; Hunt, S.W.; Leopold, K.R. Microwave investigation of sulfuric acid monohydrate. J. Am. Chem. Soc. **2002**, *124* (16), 4504–4511.
64. Ott, M.E.; Leopold, K.R. A microwave study of the ammonia–nitric acid complex. J. Phys. Chem. A **1999**, *103* (10), 1322–1328.
65. Dyke, T.R.; Mack, K.M.; Muenter, J.S. The structure of water dimer from molecular beam electric resonance spectroscopy. J. Chem. Phys. **1977**, *66* (2), 498–510.
66. Fiacco, D.L.; Leopold, K.R. Partially bound systems as sensitive probes of microsolvation: a microwave and ab initio study of $HCN\cdots HCN$–BF_3. J. Phys. Chem. A **2003**, *107* (16), 2808–2814.
67. Fiacco, D.L.; Hunt, S.W.; Leopold, K.R. Structural change at the onset of microsolvation: rotational spectroscopy of $HCN\cdots HCN$–SO_3. J. Phys. Chem. **2000**, *104* (36), 8323–8327.
68. Ruoff, R.S.; Emilsson, T.; Chuang, C.; Klots, T.D.; Gutowsky, H.S. Rotational spectra and structures of small clusters containing HCN dimer: $(HCN)_2$–Y with Y = HF, HCl, HCF_3, and CO_2. J. Chem. Phys. **1989**, *90* (8), 4069–4078.
69. Grabow, J.-U.; Heineking, N.; Stahl, W. A molecular beam microwave Fourier transform spectrometer with an electric discharge nozzle. Z. Naturforsch. **1991**, *46a*, 989–992.
70. Lida, M.; Ohshima, Y.; Endo, Y. Laboratory detection of HC_9N using a Fourier transform microwave spectrometer. Astrophys. J. Lett. **1991**, *371*, L45–L46.
71. Bevan, J.W.; Legon, A.C.; Rego, C.A.; Roach, J. The vibrational state ($10^\circ 0$) of Ar–HCl excited in a pulsed jet by a glow discharge. Rotational spectrum and lifetime. Chem. Phys. Lett. **1992**, *198* (3,4), 347–354.
72. Ohshima, Y.; Endo, Y. Structure of C_3S studied by pulsed discharge nozzle Fourier transform microwave spectroscopy. J. Mol. Spectrosc. **1992**, *153*, 627–634.
73. Sumiyoshi, Y.; Endo, Y.; Ohshima, Y. Intermolecular potential energy surface of Ar–SH($^2\pi_i$) determined by a simultaneous analysis of Ar–SH/D studied by FTMW spectroscopy. J. Mol. Spectrosc. **2003**, *222* (1), 22–30.
74. Seki, K.; Sumiyoshi, Y.; Endo, Y. Pure rotational spectra of the Ar–HN_2^+ and the Kr–HN_2^+ ionic complexes. J. Chem. Phys. **2002**, *117* (21), 9750–9757.
75. Thaddeus, P.; McCarthy, M.C. Carbon chains and rings in the laboratory and in space. Spectrochim. Acta Part A **2001**, *57* (4), 757–774.

76. Gordon, V.D.; McCarthy, M.C.; Apponi, A.J.; Thaddeus, P. Rotational spectra of sulfur–carbon chains. II. HC_5S, HC_6S, HC_7S and HC_8S and H_2C_4S, H_2C_5S, H_2C_6S and H_2C_7S. Astrophys. J. Supp. **2002**, *138*, 297–303.
77. Grabow, J.-U.; Samuel Palmer, E.; McCarthy, M.C.; Thaddeus, P. A cryogenic COBRA Fourier transform microwave spectrometer (to be published).
78. Gatehouse, B.; Müller, H.S.P.; Gerry, M.C.L. Hyperfine constants and nuclear shieldings from the microwave spectra of FBO, ClBO and FBS. J. Mol. Spectrosc. **1998**, *190*, 157–167.
79. Kukolich, S.G.; Tanjaroon, C.; McCarthy, M.C.; Thaddeus, P. Microwave spectrum of *o*-benzyne produced in a discharge nozzle. J. Chem. Phys. **2003**, *119* (8), 4353–4359.
80. Suenram, R.D.; Lovas, F.J.; Matsumura, K. Laboratory measurement of the $1_{01}-0_{00}$ transition and electric dipole moment of silicon carbide (SiC_2). Astrophys. J. Lett. **1989**, *342* (2), L103–L105.
81. Brugh, D.J.; Suenram, R.D.; Stevens, W.J. Fourier transform microwave spectroscopy of jet cooled ZrO_2 produced by laser vaporization. J. Chem. Phys. **1999**, *111* (8), 3526–3535.
82. Lesarri, A.; Suenram, R.D.; Brugh, D. Rotational spectrum of jet cooled HfO_2 and HfO. J. Chem. Phys. **2002**, *117* (21), 9651–9662.
83. Walker, K.A.; Gerry, M.C.L. Microwave Fourier transform spectroscopy of magnesium sulfide produced by laser ablation. J. Mol. Spectrosc. **1997**, *182* (1), 178–183.
84. Evans, C.J.; Gerry, M.C.L. Noble gas–metal chemical bonding? The microwave spectra, structures, and hyperfine constants of Ar–CuX (X = F, Cl, Br). J. Chem. Phys. **2000**, *112* (21), 9363–9374.
85. Evans, C.J.; Gerry, M.C.L. The microwave spectra and structures of Ar–AgX (X = F, Cl, Br). J. Chem. Phys. **2000**, *112* (3), 1321–1329.
86. Evans, C.J.; Lesarri, A.; Gerry, M.C.L. Nobel gas–metal chemical bonds. microwave spectra, geometries, and nuclear quadrupole coupling constants of Ar–AuCl and Kr–AuCl. J. Am. Chem. Soc. **2000**, *122* (25), 6100–6105.
87. Walker, N.R.; Gerry, M.C.L. Microwave spectra, geometries, and hyperfine constants of OCCuX (X = F, Cl, Br). Inorg. Chem. **2001**, *40* (24), 6158–6166.
88. Walker, N.R.; Gerry, M.C.L. Microwave spectra, geometries, and hyperfine constants of OCAgX (X = F, Cl, Br). Inorg. Chem. **2002**, *41* (5), 1236–1244.
89. Evans, C.J.; Reynard, L.M.; Gerry, M.C.L. Pure rotational spectra, structures, and hyperfine constants of OC–AuX (X = F, Cl, Br). Inorg. Chem. **2001**, *40* (24), 6123–6131.

90. Mizoguchi, A.; Ohshima, Y.; Endo, Y. Microscopic hydration of the sodium chloride ion pair. J. Am. Chem. Soc. **2003**, *125* (7), 1716–1717.
91. Campbell, E.J.; Read, W.G.; Shea, J.A. The electric dipole moments of OCHF and OCDF. Chem. Phys. Lett. **1983**, *94* (1), 69–72.
92. Emilsson, T.; Gutowsky, H.S.; de Oliveira, G.; Dykstra, C.E. Rotational patches: stark effect, dipole moment, and dynamics of water loosely bound to benzene. J. Chem. Phys. **2000**, *112* (3), 1287–1294.
93. Consalvo, D. Advances in stark effect measurements in a molecular beam Fourier transform microwave spectrometer. Rev. Sci. Instrum. **1998**, *69* (9), 3136–3141.
94. Kisiel, Z.; Kosarzewski, J.; Pietrewicz, B.A.; Pszczólkowski, L. Electric dipole moments of the cyclic trimers $(H_2O)_2HCl$ and $(H_2O)_2HBr$ from stark effects in their rotational spectra. Chem. Phys. Lett. **2000**, *325* (5,6), 523–530.
95. Schnell, M.; Banser, D.; Grabow, J.-U. Coaxially aligned electrodes for Stark effect applied in resonators (CAESAR) using a COBRA Fourier transform microwave spectrometer. Rev. Sci. Instrum. **2004**, *in press*.
96. Endo, Y.; Fuji, M. Double resonance (MODR, OODR) spectroscopy. In *Nonlinear Spectroscopy for Molecular Structure Determination*; Field, R.W., Ed.; Blackwell: Oxford, UK, 1998; 29–53.
97. Martinache, L.; Jans-Bürli, S.; Vogelsanger, B.; Kresa, W.; Bauder, A. Microwave-microwave double-resonance experiments with pulsed molecular beams in crossed Fabry–Perot cavities. Chem. Phys. Lett. **1988**, *149* (4), 424–428.
98. Martinache, L.; Ozier, I.; Bauder, A. Two photon microwave transitions within a two-level system. J. Chem. Phys. **1990**, *92* (12), 7128–7134.
99. Markov, V.N.; Xu, Y.; Jäger, W. Microwave-submillimeter wave double resonance spectrometer for the investigation of van der Waals complexes. Rev. Sci. Instrum. **1998**, *69* (12), 4061–4067.
100. Nakajima, M.; Sumiyoshi, Y.; Endo, Y. Development of microwave-optical double-resonance spectroscopy using a Fourier-transform microwave spectrometer with a pulsed laser. Rev. Sci. Instrum. **2002**, *73* (1), 165–171.
101. Douglass, K.O.; Keske, J.C.; Rees, F.S.; Welch, K.; Yoo, H.S.; Pate, B.H.; Leonov, I.; Suenram, R.D. Rotational spectroscopy of vibrationally excited states by infrared-Fourier transform microwave-microwave triple-resonance spectroscopy. Chem. Phys. Lett. **2003**, *376* (5,6), 548–556.
102. Jäger, W.; Xu, Y.; Gerry, M.C.L. Pure rotational spectra of the mixed rare gas van der Waals complexes Ne–Xe, Ar–Xe and Kr–Xe. J. Chem. Phys. **1993**, *99* (2), 919–927.

103. Xu, Y.; Jäger, W.; Djauhari, J.; Gerry, M.C.L. Rotational spectra of the mixed rare gas dimers Ne–Kr and Ar–Kr. J. Chem. Phys. **1995**, *103* (8), 2827–2833.
104. Xu, Y.; Jäger, W.; Gerry, M.C.L. Microwave spectroscopic investigation of the mixed rare gas van der Waals trimers Ne_2–Kr and Ne_2–Xe. J. Chem. Phys. **1994**, *100* (6), 4171–4180.
105. Grabow, J.-U.; Pine, A.S.; Fraser, G.T.; Lovas, F.J.; Suenram, R.D.; Emilsson, T.; Arunan, E.; Gutowsky, H.S. Rotational spectra and van der Waals potentials of Ne–Ar. J. Chem. Phys. **1995**, *102* (3), 1181–1187.
106. Xu, Y.; Jäger, W. High resolution spectroscopy of Ne and Ar containing noble gas clusters. J. Chem. Phys. **1997**, *107* (13), 4788–4796.
107. Ernesti, A.; Hutson, J.M. Calculations of spectra of rare gas dimers and trimers: implications for additive and non-additive intermolecular forces in Ne_2–Ar, Ne_2–Kr, Ne_2–Xe, Ar_2–Ne, Ar_3, Ar_2–Kr, and Ar_2–Xe. J. Chem. Phys. **1995**, *103* (9), 3386–3391.
108. Gutowsky, H.S.; Emilsson, T.; Arunan, E. Rotational spectra, structure and internal dynamics of Ar–H_2S isotopomers. J. Chem. Phys. **1997**, *106* (13), 5309–5315.
109. de Oliveira, G.; Dykstra, C.E. The weak interaction potential of Ar–H_2S. J. Chem. Phys. **1997**, *106* (13), 5316–5323.
110. de Oliveira, G.; Dykstra, C.E. Anomalous isotope effect in Ar–H_2S versus the normal isotope effect in Ne–H_2S. J. Chem. Phys. **1999**, *110* (1), 289–295.
111. Liu, Y.; Jäger, W. Rotational spectra and internal dynamics of Ne–H_2S. Mol. Phys. **2002**, *100* (5), 611–622.
112. Xu, Y.; Jäger, W. Spectroscopic investigation of weak interactions in the van der Waals trimer $NeArCO_2$. Mol. Phys. **1998**, *93* (5), 727–737.
113. McKellar, A.R.W.; Xu, Y.; Jäger, W.; Bissonnette, C. Isotopic probing of very weak intermolecular forces: microwave and infrared spectra of CO–He isotopomers. J. Chem. Phys. **1999**, *110* (22), 10766–10773.
114. Xu, Y.; Jäger, W. Rotational spectroscopic investigation of carbonyl sulfide solvated with helium atoms. J. Chem. Phys. **2003**, *119* (11), 5457–5466.
115. Xu, Y.; Jäger, W.; Tang, J.; McKellar, A.R.W. Spectroscopic studies of quantum solvation in He_n–N_2O clusters. Phys. Rev. Lett. **2003**, *91* (16), 163401/1–163401/4.
116. Peebles, R.A.; Kuczkowski, R.L. The OCS trimer: isotopic studies, structure, and dipole moment. J. Phys. Chem. A **1999**, *103* (32), 6344–6350.
117. Arunan, E.; Gutowsky, H.S. The rotational spectrum, structure, and dynamics of a benzene dimer. J. Chem. Phys. **1993**, *98* (5), 4294–4296.

118. Sinnokrot, M.O.; Valeev, E.F.; Sherrill, C.D. Estimates of the ab initio limit for $\pi-\pi$ interactions: the benzene dimer. J. Am. Chem. Soc. **2002**, *124* (36), 10887–10893.
119. Goly, T.; Spoerel, U.; Stahl, W. The microwave spectrum of the 1,2-difluorobenzene dimer. Chem. Phys. **2002**, *283* (1,2), 289–296.
120. Arunan, E.; Emilsson, T.; Gutowsky, H.S.; Fraser, G.T.; de Oliveira, G.; Dykstra, C.E. Rotational spectrum of the weakly bonded $C_6H_6-H_2S$ dimer and comparisons to $C_6H_6-H_2S$ dimer. J. Chem. Phys. **2002**, *117* (21), 9766–9776.
121. Gutowsky, H.S.; Emilsson, T.; Arunan, E. Low-J rotational spectra, internal rotation, and structures of several benzene–water dimers. J. Chem. Phys. **1993**, *99* (7), 4883–4893.
122. Rodham, D.A.; Suzuki, S.; Suenram, R.D.; Lovas, F.J.; Dasgupta, S.; Goddard, W.A. III; Blake, G.A. Hydrogen bonding in the benzene-ammonia dimer. Nature **1993**, *362*, 735–737.
123. Sanz, M.E.; Antolinez, S.; Alonso, J.L.; Lopez, J.C.; Kuczkowski, R.L.; Peebles, S.A.; Peebles, R.A.; Boman, F.C.; Kraka, E.; Cremer, D. The microwave spectrum, ab initio analysis, and structure of the fluorobenzene–hydrogen chloride complex. J. Chem. Phys. **2003**, *118* (20), 9278–9290.
124. Mäder, H.; Brendel, K.; Jäger, W. The microwave spectra of flourobenzne–H_2O and 1,4-difluorobenzene–H_2O and internal rotation analysis, 57th International Symposium on Molecular Spectroscopy 2002, Abstract No. TJ14.
125. Read, W.G.; Campbell, E.J.; Henderson, G. The rotational spectrum and molecular structure of the benzene–hydrogen chloride complex. J. Chem. Phys. **1983**, *78* (6, part 2), 3501–3508.
126. Tarakeshwar, P.; Kim, K.S.; Brutschy, B. Fluorobenzene–water and difluorobenzene–water systems: an ab initio investigation. J. Chem. Phys. **1999**, *110* (17), 8501–8512.
127. Peebles, S.A.; Kuczkowski, R.L. Rotational spectrum and internal motions of the ethylene–OCS weakly bound dimer. Mol. Phys. **2001**, *99* (3), 225–237.
128. Peebles, R.A.; Peebles, S.A.; Kuczkowski, R.L. Rotational spectrum and structure of the $(OCS)_2-C_2H_4$ trimer: example of a polar OCS dimer. J. Mol. Struct. **2002**, *612* (2–3), 261–275.
129. Randall, R.W.; Wilkie, J.M.; Howard, B.J.; Muenter, J.S. Infrared vibration-rotation spectrum and structure of the carbonyl sulfide dimer. Mol. Phys. **1990**, *69* (5), 839–852.
130. Peebles, S.A.; Kuczkowski, R.L. Rotational spectrum and structure of $(OCS)_2-CO_2$ trimer. J. Phys. Chem. A **1998**, *102* (42), 8091–8096.

131. Peebles, S.A.; Kuczkowski, R.L. Rotational spectrum and modeling of the OCS–$(HCCH)_2$ trimer. Theochem. **2000**, *500*, 391–402.
132. Leung, H.O.; Ibidapo, O.M.; Abruna, P.I.; Bianchi, M.B. Nuclear quadrupole hyperfine coupling interactions in the rotational spectra of the linear and bent isomers of HF–N_2O. J. Mol. Spectrosc. **2003**, *222* (1), 3–14.
133. Fraser, G.T.; Xu, L.-H.; Suenram, R.D.; Lugez, C.L. Rotational spectra of four of the five conformers of 1-pentene. J. Chem. Phys. **2000**, *112* (14), 6209–6217.
134. Fraser, G.T.; Suenram, R.D.; Lugez, C.L. Rotational spectra of seven conformational isomers of 1-hexene. J. Phys. Chem. A **2000**, *104* (6), 1141–1146.
135. Fraser, G.T.; Suenram, R.D.; Lugez, C.L. Investigation of conformationally rich molecules: rotational spectra of fifteen conformational isomers of 1-octene. J. Phys. Chem. A **2001**, *105* (43), 9859–9864.
136. Lavrich, R.J.; Farrar, J.O.; Tubergen, M.J. Heavy-atom structure of alaninamide from rotational spectroscopy. J. Phys. Chem. A **1999**, *103* (24), 4659–4663.
137. Kuhls, K.A.; Centrone, C.A.; Tubergen, M.J. Microwave spectroscopy of the twist C^{β}-Exo/C^{γ}-Endo conformation of prolinamide. J. Am. Chem. Soc. **1998**, *120* (39), 10194–10198.
138. Lavrich, R.J.; Trook, C.R.; Tubergen, M.J. Effect of the bulky side chain on the backbone structure of the amino acid derivative valinamide. J. Phys. Chem. A **2002**, *100* (35), 8013–8018.
139. Lavrich, R.J.; Plusquellic, D.F.; Suenram, R.D.; Fraser, G.T.; Walker, A.R.H.; Tubergen, M.J. Experimental studies of peptide bonds: identification of the C_7^{eq} conformation of the alanine dipeptide analog *N*-acetylalanine *N*′-methylamide from torsion-rotation interactions. J. Chem. Phys. **2003**, *118* (3), 1253–1265.
140. Sanz, M.E.; Lopez, J.C.; Alonso, J.L. Axial and equatorial hydrogen bonds in pentamethylene sulfide$\cdots$hydrogen chloride complex. Chem. Eur. J. **1999**, *5* (11), 3293–3298.
141. Blanco, S.; Lesarri, A.; Lopez, J.C.; Alonso, J.L. Axial and equatorial hydrogen bonds: jet-cooled rotational spectrum of the pentamethylene sulfide-hydrogen fluoride complex. Chem. Eur. J. **2002**, *8* (7), 1603–1613.
142. Antolinez, S.; Lopez, J.C.; Alonso, J.L. Axial and equatorial hydrogen bonds in the tetrahydropyran$\cdots$HCl dimer. Angew. Chem. Int. Ed. **1999**, *38* (12), 1772–1774.
143. Antolinez, S.; Lopez, J.C.; Alonso, J.L. The axial and equatorial hydrogen bonds in the tetrahydropyran$\cdots$HF complex. Chem. Phys. Chem. **2001**, *2* (2), 114–117.

144. Sanz, M.E.; Lopez, J.C.; Alonso, J.L. Axial and equatorial hydrogen-bond conformers and ring-puckering motion in the trimethylene sulfide-hydrogen fluoride complex. Chem. Eur. J. **2002**, *8* (18), 4265–4271.
145. Ruoff, R.S.; Klots, T.D.; Emilsson, T.; Gutowsky, H.S. Relaxation of conformers and isomers in seeded supersonic jets and inert gases. J. Chem. Phys. **1990**, *93* (5), 3142–3150.
146. Lambert, J.B.; Keske, R.G.; Weary, D.K. Conformational characterization of simple group VI heterocycles. J. Am. Chem. Soc. **1967**, *89* (23), 5921–5924.
147. Lesarri, A.; Mata, S.; Lopez, J.C.; Alonso, J.L. A laser-ablation molecular-beam Fourier-transform microwave spectrometer: the rotational spectrum of organic solids. Rev. Sci. Instrum. **2003**, *74* (11), 4799–4804.
148. Lesarri, A.; Mata, S.; Cocinero, E.J.; Blanco, S.; Lopez, J.C.; Alonso, J.L. The structure of neutral proline. Angew. Chem. Int. Ed. **2002**, *41* (24), 4673–4676.
149. Tatamitani, Y.; Liu, B.; Shimada, J.; Ogata, T.; Ottaviani, P.; Maris, A.; Caminati, W.; Alonso, J.L. Weak, improper, C–O···H–C hydrogen bonds in the dimethyl ether dimer. J. Am. Chem. Soc. **2002**, *124* (11), 2739–2743.
150. van der Waaken, B.J.; Herrebout, W.A.; Szostak, R.; Shchepkin, D.N.; Havlas, Z.; Hobza, P. The nature of improper, blue-shifting hydrogen bonding verified experimentally. J. Am. Chem. Soc. **2001**, *123* (49), 12290–12293.
151. Hermansson, K. Blue-shifting hydrogen bonds. J. Phys. Chem. A **2002**, *106* (18), 4695–4702.
152. King, A.K.; Howard, B.J. A high-resolution microwave study of the conformations of butan-2-ol in a supersonic expansion. J. Mol. Spectrosc. **2001**, *205* (1), 38–42.
153. King, A.K.; Howard, B.J. A microwave study of the hetero-chiral dimer of butan-2-ol. Chem. Phys. Lett. **2001**, *348* (3,4), 343–349.
154. Blanco, S.; Whitham, C.J.; Qian, H.; Howard, B.J. A microwave study of the open-shell complex Kr–NO_2. Phys. Chem. Chem. Phys. **2001**, *3* (18), 3895–3900.
155. Mandal, P.K.; Arunan, E. Hydrogen bond radii for the hydrogen halides and van der Waals radius of hydrogen. J. Chem. Phys. **2001**, *114* (9), 3880–3882.
156. Gadre, S.R.; Bhadane, P.K. Patterns in hydrogen bonding via electrostatic potential topography. J. Chem. Phys. **1997**, *107* (14), 5625–5626.
157. Samuelson, A.G.; Arunan, E. (to be published).
158. Karan, N.K.; Arunan, E. Chlorine bond distances in ClF and Cl_2 complexes. J. Mol. Struct. **2003**, *688*, 235–237.

159. Meyer, Vo.; Sutter, D.H.; Dreizler, H. The centrifugally induced pure rotational spectrum and the structure of sulfur trioxide. A microwave Fourier transform study of a nonpolar molecule. Z. Naturforsch. **1991**, *46a*, 710–714.
160. Oldani, M.; Ha, T.-K.; Bauder, A. Deuterium nuclear quadrupole hyperfine coupling in benzen-D_1 observed by pulsed microwave Fourier transform spectroscopy. Chem. Phys. Lett. **1985**, *115* (3), 317–320.
161. Brupbacher, Th.; Lüthi, H.P.; Bauder, A. An ab initio investigation of the potential energy surface of the benzene–neon van der Waals complex. Chem. Phys. Lett. **1992**, *195* (5,6), 482–486.
162. Arunan, E.; Emilsson, T.; Gutowsky, H.S. Rotational spectrum and structure of $Ne–C_6H_6–H_2O$, an aromatic sandwich. J. Chem. Phys. **1993**, *99* (8), 6208–6210.
163. Gutowsky, H.S.; Arunan, E.; Emilsson, T.; Tschopp, S.L.; Dykstra, C.E. Rotational spectra and structures of the $C_6H_6–HCN$ dimer and $Ar_3–HCN$ tetramer. J. Chem. Phys. **1995**, *103* (10), 3917–3927.
164. Gutowsky, H.S.; Klots, T.D.; Chuang, C.; Schmuttenmaer, C.A.; Emilsson, T. Rotational spectra and structures of $Ar_2–HF/DF$ trimers. J. Chem. Phys. **1987**, *86* (2), 569–576.
165. Klots, T.D.; Chuang, C.; Ruoff, R.S.; Emilsson, T.; Gutowsky, H.S. Rotational spectra and structures of $Ar_2–HCl/DCl$ trimers. J. Chem. Phys. **1987**, *86* (2), 5315–5322.
166. Kisiel, Z.; Pietrewicz, B.A.; Pszczólkowski, L. The observation and characterization of the weakly bound trimer $Ar_2–HBr$. J. Chem. Phys. **2002**, *117* (18), 8248–8255.
167. Arunan, E.; Dykstra, C.E.; Emilsson, T.; Gutowsky, H.S. Rotational spectra, structures and dynamics of small $Ar_m–(H_2O)_n$ clusters: the Ar_2-H_2O trimer. J. Chem. Phys. **1996**, *105* (19), 8495–8501.
168. Mandal, P.K.; Arunan, E. Rotational spectra and structure of Ar_2-H_2S complex: FT microwave spectroscopic and ab initio studies, 58th International Symposium on Molecular Spectroscopy, Columbus, June 16–20, 2003; Abstract No. MH03.
169. Gutowsky, H.S.; Klots, T.D.; Dykstra, C.E. Rotational spectrum and potential surface for $Ar_2–HCN$: a T-shaped cluster with internal rotation. J. Chem. Phys. **1990**, *93* (9), 6216–6225.
170. Arunan, E.; Emilsson, T.; Gutowsky, H.S. Rotational spectra, structures and dynamics of small $Ar_m–(H_2O)_n$ clusters: the $Ar–(H_2O)_2$ trimer. J. Chem. Phys. **2002**, *116* (12), 4886–4895.
171. Fraser, G.T. $(H_2O)_2$: spectroscopy, structure, and dynamics. Int. Rev. Phys. Chem. **1991**, *10* (2), 189–206.

172. Kisiel, Z.; Bialkowska-Jaworska, E.; Pszczolkowski, L.; Milet, A.; Struniewicz, C.; Moszynski, R.; Sadlej, J. Structure and properties of the weakly bound trimer $(H_2O)_2HCl$ observed by rotational spectroscopy. J. Chem. Phys. **2000**, *112* (13), 5767–5776.
173. Kisiel, Z.; Pietrewicz, B.A.; Desyatnyk, O.; Pszczolkowski, L.; Struniewicz, I.; Sadlej, J. Structure and properties of the weakly bound cyclic trimer $(H_2O)_2$ HBr observed by rotational spectroscopy. J. Chem. Phys. **2003**, *119* (12), 5907–5917.
174. Arunan, E.; Emilsson, T.; Gutowsky, H.S. Rotational spectra, structure, and dynamics of $Ar_m–(H_2O)_n$ clusters: $Ar_2–H_2O$, $Ar_3–H_2O$, $Ar–(H_2O)_2$, and $Ar–(H_2O)_3$. J. Am. Chem. Soc. **1994**, *116* (18), 8418–8419.
175. Keutsch, F.N.; Cruzan, J.D.; Saykally, R.J. The water trimer. Chem. Rev. **2003**, *103* (7), 2533–2577.
176. Chen, W.; Hight Walker, A.R.; Novick, S.E.; Tao, F-M. Determination of the structure of HBr–DBr. J. Chem. Phys. **1997**, *106* (15), 6240–6247.
177. Howard, B.J. unpublished results as quoted in 176.
178. Arunan, E. Assuming the *A* for Ar-$(HF)_2$ to be very close to the *B* for $(HF)_2$ yielded several transitions which remain unassigned (unpublished results).
179. Klemeperer, W. Some spectroscopic reminiscences. Ann. Rev. Phys. Chem. **1995**, *46*, 1–28.
180. Tatamitani, Y.; Ogata, T. Intermolecular hydrogen bonds, rotational spectrum, and structure of van der Waals complexes $(CH_3)_2O\cdots CF_2{=}CH_2$ and $(CH_3)_2O\cdots CF_2{=}CHF$. J. Mol. Spectrosc. **2003**, *222* (1), 102–108.

ARTICLE INFORMATION SHEET: Contact or Corresponding Author		
	CMS ID number (DOI):	120030906
	Article title:	Pulsed Nozzle Fourier Transform Microwave Spectrometer: Advances and Applications
	Article type:	Research
	Classification: Category:	
	Primary subcategory:	
	Subcategpry(ies):	
	Topic(s):	
	Key words:	FTMW spectroscopy; van der Waals complexes; Hydrogen bonding; Electrophore
	Copyright holder:	
	Author Sequence Number	1
	Author first name or first initial:	E.
	Author middle initial:	
	Author last name:	Arunan
	Suffix to last name:	
	Degrees:	
	Author Status	
	Author e-mail address:	earunan@rediffmail.com
	Author fax:	+91-80-2360-1552
	Author phone:	
Primary Affiliation(s) at time of authorship:	*Title or Position*	
	Department(s)	Department of Inorganic and Physical Chemistry
	Institution or Company	Indian Institute of Science
	Domestic (U.S.A.) or International	International
	Suite, floor, room no.	
	Street address	
	City	Bangalore
	State/Province	
	Postal code	560 012
	Country	India
Secondary Affiliation(s) at time of authorship:	*Title or Position*	
	Department(s)	
	Institution or Company	
	Domestic (U.S.A.) or International	
	Suite, floor, room no.	
	Street address	
	City	
	State/Province	
	Postal code	
	Country	
Current affiliation(s):	*Title or Position*	
	Department(s)	
	Institution or Company	
	Suite, floor, room no.	
	Street address	
	City	
	State/Province	
	Postal code	
	Country	
Mailing address:	*Department(s)*	
	Institution or Company	
	Street address	
	Suite, floor, room no.	
	City	
	State/Province	
	Postal code	
	Country	
Recipient of R1 proofs:	*e-mail address to receive proofs:*	earunan@rediffmail.com
	Fax to receive proofs:	+91-80-2360-1552
	Mailing address to receive proofs:	
Article data:	*Submission date:*	
	Reviewed date:	
	Revision date:	
	Accepted date:	